



JEM/SMILES Level-2 Product Guide for v2.4 (008-11-0502)

Draft 0.1

July 3, 2013



This page is blank to preserve correct left-right pagination



JEM/SMILES L2 Products Guide

Table of Contents

Preface			. 4
1. Pui	rpose	of the document	. 5
2. SM	ILES	S observation and data processing	6
2.1.	Intr	roduction to SMILES	6
2.2.	SM	ILES observation	9
2.3.	The	SMILES ground data system	12
2.4.	Con	nparison method	13
2.5.	A pı	riori dataset	14
2.6.	Pro	duct release calendar	15
3. Lat	est u	pdates for SMILES L2 products	17
3.1.	Sun	nmary of algorithm updates	17
3.2.	Use	ful data	18
3.3.	Pro	file differences between v2.4 and v2.1	18
3.3	.1	O ₃	18
3.3	.2	HCl	21
3.3	.3	ClO	22
3.3	.4	HNO ₃	24
3.3	.5	HOC1	26
3.3	.6	CH ₃ CN	28
3.3	.7	BrO	29
3.3	.8	HO_2	31
3.3	.9	Temperature	33
3.3	.10	O_3 isotopes	34
3.4.	Ren	naining Issues	37
4. SM	ILES	S L2 products	38
4.1.	Def	inition of data products	38
4.2.	L2	products overview	38
4.3.	Dat	a screening	39
4.4.	Pro	duct format	39
Referen	ices		45
Append	ix		48

JEM/SMILES L2 Product Guide for v2.4



A. 1.	Information in previous versions	48
A. 1	. 1. Description of v1.0 (005-06-0024)	48
A. 1	. 2. Improvements in v 1.1 (005-06-0032) update	48
A. 1	. 3. Improvements in v 1.2 (005-06-0150) update	48
A. 1	. 4. Improvements in v 1.3(006-06-0200) update	49
A. 1	. 5. Improvements in v 2.0 (007-08-0300) update	50
A. 1	. 6. Improvements in v 2.1(007-08-0310) update	52
A. 1	. 7. Improvements in v 2.2 (007-09-0400) update	52
A. 1	. 8. Improvements in v 2.3 (007-09-0402) update	54
A. 1	. 9. Improvements in v 2.4 (008-11-0502) update	54
Δ 9	Sample of source code for reading L2 product (in python)	6.



PREFACE

The Superconducting Submillimeter-Wave Limb-Emission Sounder (SMILES) was developed for use aboard the Japanese Experiment Module (JEM) on the International Space Station (ISS) through the cooperation of the Japan Aerospace Exploration Agency (JAXA) and the National Institute of Information and Communications Technology (NICT). SMILES was successfully launched on an H-IIB rocket with an H-II Transfer Vehicle on 11 September, 2009, was attached to the JEM on 25 September, and began atmospheric observations on 12 October. Mission objectives are as follows: (1) to demonstrate a 4 K mechanical cooler and superconducting mixers in the environment of outer space for submillimeter limb-emission sounding in the frequency bands of 624.32-626.32 GHz and 649.12-650.32 GHz and (2) to globally measure minor atmospheric constituents in the middle atmosphere (O₃, HCl, ClO, HO₂, HOCl, BrO, O₃ isotopes, HNO₃, CH₃CN, etc.) to gain a better understanding of factors and processes controlling the amount of stratospheric ozone and the relationship with climate change. Unfortunately, SMILES observations have been suspended since 21 April 2010 owing to the failure of a critical component in the submillimeter local oscillator. Although the observation period was limited to about six months, SMILES had been performing global observations at about 100 locations per ISS orbit, except for some restrictions due to ISS operation. After data processing, we had global and vertical distributions of about 10 minor atmospheric constituents related to ozone chemistry. In this document we will demonstrate the capability of obtaining high-quality scientific data which will be important in addressing scientific issues such as the ozone depletion problem, middle atmosphere chemistry with a special focus on the diurnal cycle, and the transport process for minor species. We hope the output from SMILES will demonstrate its high potential to observe minor atmospheric constituents in the middle atmosphere.

Masato Shiotani

Principle Investigator of the SMILES mission team



1. Purpose of the document

Researchers and scientists in atmospheric sciences can use this document to understand the quality and characteristics of the data from Superconducting Submillimeter-wave Limb-emission Sounder (SMILES) on the basis of SMILES standard level 2 (L2) products processed and provided by JAXA.

This product guide provides the following:

- 1) Descriptions of SMILES observations.
- 2) Descriptions of the latest SMILES L2 products.
- 3) Descriptions of data format.



2. SMILES OBSERVATION AND DATA PROCESSING

2.1. Introduction to SMILES

The Superconducting Submillimeter-wave Limb-Emission Sounder (SMILES) was launched on September 11, 2009 as a joint project between the Japan Aerospace Exploration Agency (JAXA) and the National Institute of Information and Communications Technology (NICT), and was attached to the Japanese Experiment Module (JEM) on the International Space Station (ISS) on September 25, 2009. For details of SMILES configurations, see the SMILES Mission Plan, version 2.1, at http://darts.isas.jaxa.jp/iss/smiles/docs/SMILES_MP_ver2-1.pdf. SMILES carries 4 K cooled Superconductor-Insulator-Super-conductor (SIS) mixers to carry out high-sensitivity measurements for submillimeter limb-emission sounding. Since the system noise temperature of SMILES is nearly 350 K, the sensitivity of SMILES is much higher than that of similar sensors in orbit. For general post-launch information, you may consult Kikuchi et al. (2010); some important information on SMILES measurement is summarized in Table 2.2-1.

SMILES measures atmospheric limb emission from minor constituents within the submillimeter-wave region from 625 GHz to 650 GHz for three specified detection bands: 624.32–625.52 GHz (Band A), 625.12–626.32 GHz (Band B), and 649.12–650.32 GHz (Band C). Target species and sample spectra are shown in Table 2.1-1 and Figure 2.1-2 respectively. SMILES instruments only consist of two AOS spectrometers. Accordingly, observations of Bands A, B, and C are made on a time-sharing basis. Depending on the combination, the AOS spectrometer for Band A may be switched.

Table 2.1-1 Major characteristics of SMILES [Ochiai et al., 2012]

System parameter	Description
Frequency bands	624.26 - 625.59 GHz (Band A)
	625.06 – 626.38 GHz (Band B)
	649.05 - 650.38 GHz (Band C)
Frequency resolution	1.05 1.20 MHz (FWHM)
Number of channels	1728 for each unit of AOS
Channel separation	approx. 0.8 MHz
Integration time	0.47 s for each observation point
Calibration period	53 s



System parameter	Description
System noise temperature	297 - 380 K
Temperature resolution	0.30 - 0.42 K (for line spectrum)
	0.18 - 0.27 K (for continuum)
Beam width	0.089 deg.(V) x 0.173 deg. (H) (FWHM)

Table 2.1-2 SMILES target species in level-2 data processing

Band	Band A	Band B	Band C
	(624.32–625.52GHz)	(625.12–626.32GHz)	(649.12-650.32GHz)
Target Species	O_3	O_3	O_3
	HCl (H ³⁷ Cl)	HCl (H ³⁵ Cl)	ClO
	¹⁸ OOO	¹⁸ OOO	HNO_3
	HNO ₃	$O^{17}OO$	¹⁸ OOO
	CH ₃ CN	HO_2	¹⁷ OOO
	HOCl		HO_2
	$O^{17}OO$		BrO
	BrO		



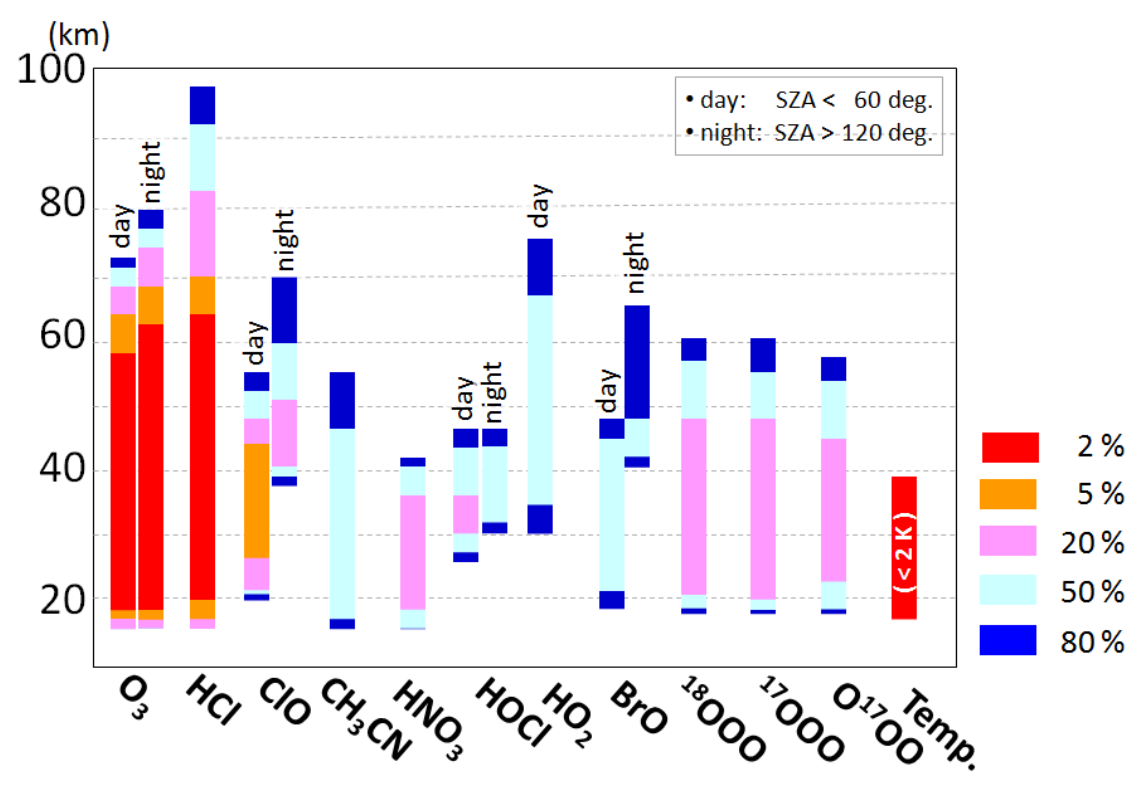
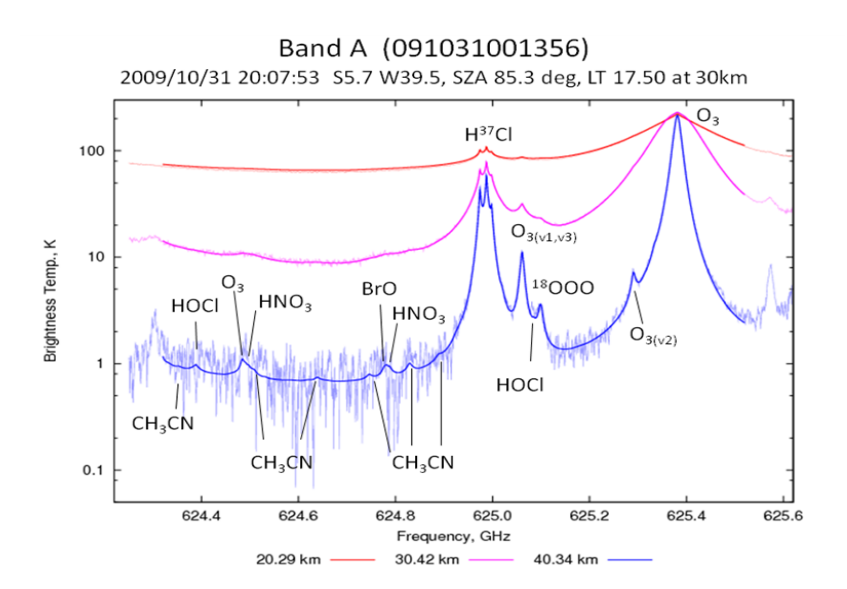


Figure 2.1-1 Theoretical precision ratios (single scan) by *a priori* profile (March 2010, Northern middle-latitude).





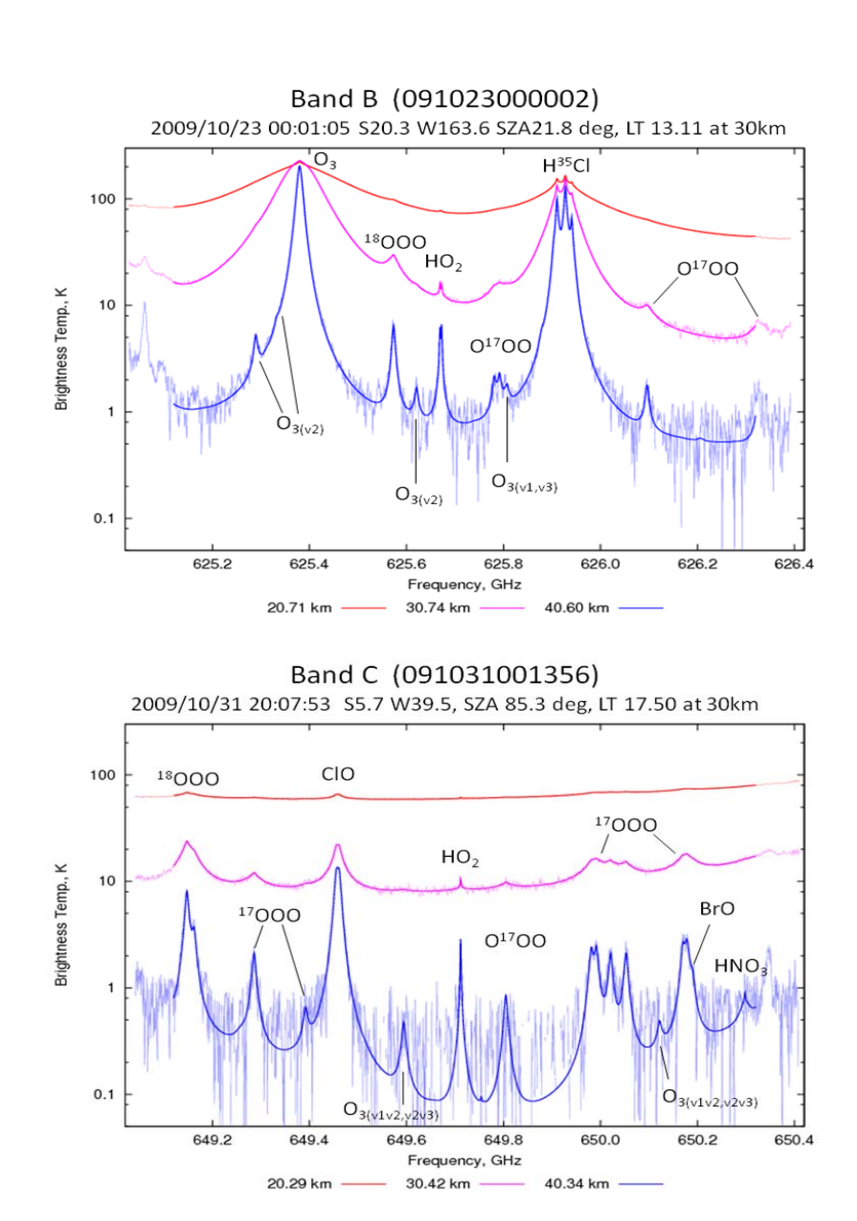


Figure 2.1-1: Samples of observed and fitted spectra (thin lines: observed, thicklines: fitted) in each band [Suzuki et al., 2012]

2.2. SMILES OBSERVATION

The ISS has a circular orbit with an inclination angle of 51.6°, and is located at an altitude of about 400 km above the Earth's surface. While it circles the Earth at 90 minutes per orbit, atmospheric observations are being conducted. The SMILES antenna is tilted 45° to the left from the direction of orbital motion. This design enables SMILES to observe latitudes from 38° S to 65° N.

Figure 2.2-1 shows an example of globally mapped ozone distribution at 28 km on 20 March, 2010. Original observation points are plotted using white circles with observed ozone mixing ratios.



White circles without color indicate missing data points rejected as abnormal values. It was discovered that SMILES performed observations continuously, but we can see that there are specific latitudes where the data is missing. This is due to solar paddle interference that occurred twice in one circular orbit.

The observation period was from October 12, 2009 to April 21, 2010. The first few weeks until November 6 were used as a trial period before going into full SMILES operational mode. During this period, the ratio of missing data was quite high. In addition, the AOS thermal control heaters were turned off gradually therefore we need to be careful of differing characteristics in SMILES data in the trial compared with the following observation period. Details of data availability, its quality, and valid latitude range are summarized in Table 2.2-1 and Figure 2.2-2.

Another important aspect of SMILES observations is that SMILES can measure the atmosphere at different local times because of the non-sun-synchronous ISS orbit. ISS local time precession takes about two months to cover the whole day therefore we may calculate diurnal variations by combining the data from the ascending and descending nodes on the basis of a one month period approximately (Figure 2.2-3).

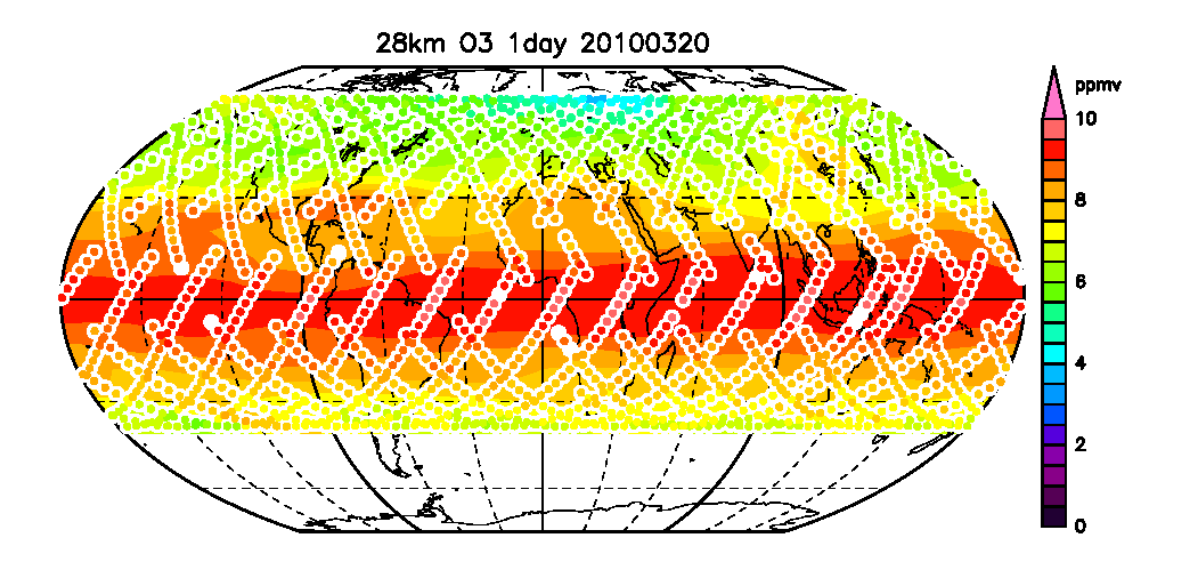


Figure 2.2-1 Measurement positions for 1day

Table 2.2-1 Irregular data from SMILES L2 product

Period	Event	Data number	Ratio of un-useable scans	Latitude coverage
2009/10/12 - 11/06	Trial period	almost	almost	normal
		normal	normal	



Period	Event	Data number	Ratio of un-useable scans	Latitude coverage
2009/10/12 – 23	AOS thermal control heaters turned on.	-	-	-
2009/10/24 – 26	Some AOS thermal control heaters turned on.	-	-	1
2009/10/27 –	AOS thermal control heaters turned off.	-	-	1
2009/11/19 – 11/24	ISS yaw maneuver (Atlantis docking)	normal	normal	opposite direction
2009/11/30 – 12/15	ISS solar paddles stopped just in front of SMILES IFOV ¹	normal	high	normal
2010/02/10 09:00 - 2010/02/19 23:59	ISS yaw maneuver (Endeavour docking)	normal	normal	opposite direction
2010/02/24 00:00 - 2010/03/05 15:00	Trouble with ISS/JEM communication system	low (10% of normal level)	normal	normal
2010/04/07 11:00 - 2010/04/17 11:59	ISS yaw maneuver (Discovery docking)	normal	normal	opposite direction

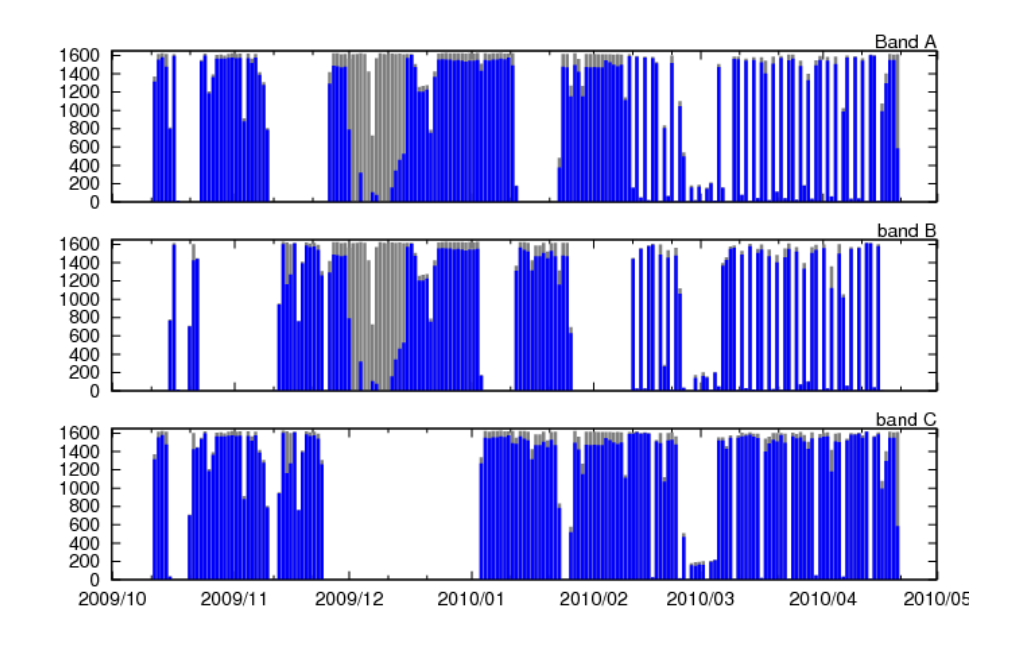


Figure 2.2-2 Observation numbers per day for Bands A, B, and C. Gray regions show total observations; blue regions show available numbers after discarding abnormal scans such as those due to field obstacles indicated by L1B information (L1B 008).

_

due to maintenance on ISS Port Solar Alpha Rotary Joint Elements



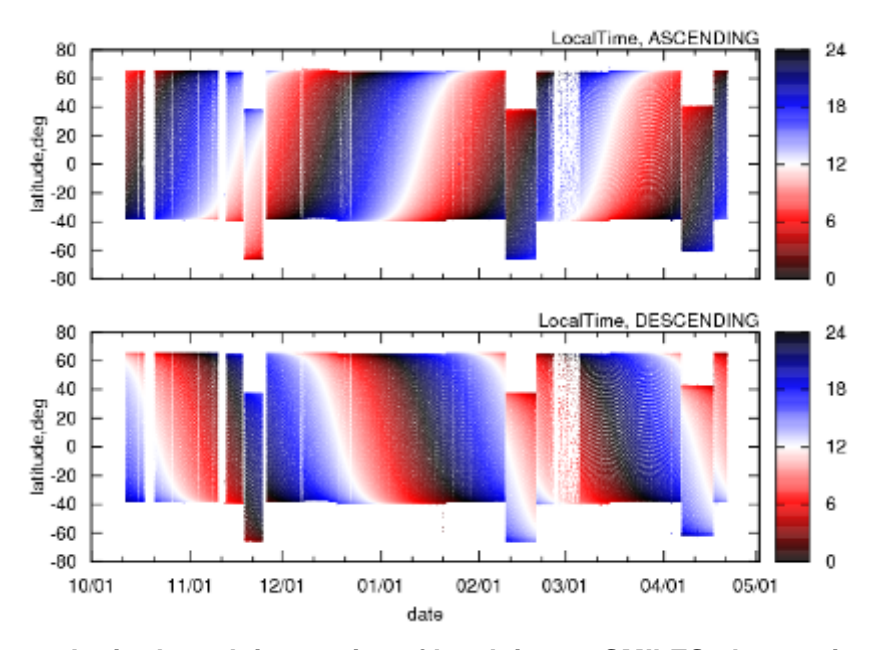


Figure 2.2-1 Latitude and time series of local time at SMILES observation points.

2.3. SMILES GROUND DATA SYSTEM

Data observed by SMILES is multiplexed with data from other JEM experiments. Multiplexed data is downlinked from the ISS through geostationary data relay satellites to ground receiving stations. SMILES data is processed from RAW data to L0 data at the User Operation Area at JAXA/TKSC. SMILES L0 data is provided to the DPS-L0/L1 Data Processing System for the SMILES Ground Data System.

L0 data is converted into calibrated limb spectral radiance using calibration data in the L0/L1 data processing system (DPS-L0/L1). Anomalous data is checked and flagged before processing. Ancillary data such as tangent altitude and position of the observation are created and added as a part of L1 data products. L1 data is transferred to the L2 Data processing system (DPS-L2) via the network and converted into L2 data which consists of concentration profiles of targeted gases, temperature and pressure. Standard L2 data processing is performed at JAXA/ISAS.



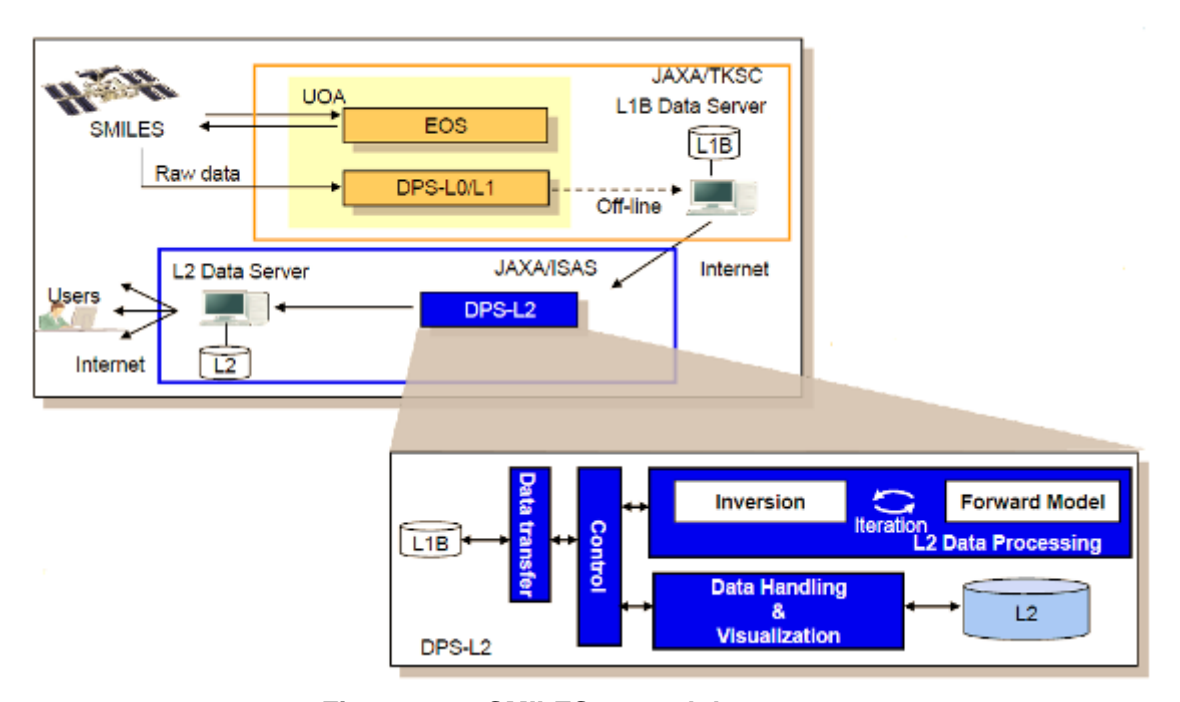


Figure 2.2-1 SMILES ground data system

2.4. COMPARISON METHOD

This section explains the comparison method for SMILES data and other datasets (such as ozonesonde data). To compare two correlative profiles with different vertical resolutions, vertical resolution should be adjusted with averaging kernels. Other transformed data \mathfrak{F} is defined

$$\tilde{\mathbf{x}} = \mathbf{A}\mathbf{x} + (\mathbf{I} - \mathbf{A})\mathbf{x}^{\mathbf{a}},$$

where **I** is the unit matrix, **A** is the SMILES averaging kernel, and \mathbf{x}^a is the SMILES a priori profile. The difference between SMILES data (\mathbf{x}) and the data of other sensors (\mathbf{x}^{*}), δ , is

$$\delta = x - \tilde{x} = (x - x) + (I - A)(x - x^a)$$

Here we will skip the explanation of the SMILES retrieval algorithm. It is based on the optimal estimation method (Rodgers, 1976, 2000). The details of the retrieval algorithm for the DPS-L2 can be found in a separate technical paper (Takahashi et al., 2009).



2.5. A PRIORI DATASET

For operational L2 processing, we prepared 7 sets of a priori data calculated from 5 data sources including satellite data, reanalysis data, and output from chemistry transport models (Table 2.5-1, Table 2.5-2).

Table 2.5-1 A priori datasets

Table 2.5 1 A priori datasets				
Data set	Description			
Climatology				
Aura/MLS	Monthly average for 2005-2007 from EOS-Aura/MLS v2.2 [Froidevaux et al., 2008]. Latitude bin is 10 degrees, and day-time and night-time sets were prepared separately for O ₃ ,ClO, HOCl, HO ₂ , BrO.			
UARS/MLS	Monthly average for 1992-1994 from UARS/MLS. Latitude bin is 10 degrees.			
CCSR/NIES	Monthly average of CCMVal-REF2 output for 2001-2010 from CCSR/NIES CCM [<i>Akiyoshi et al.</i> , 2009, 2010]. Latitude bin is 10 degrees, and hourly sets in local time were prepared for O ₃ , ClO, HOCl, HO ₂ , BrO.			
SD-WACCM	Monthly average for same month from SD-WACCM CCM [Kunz et al., 2011] nudged with GEOS-5. Latitude bin is 1.8 degrees, and hourly sets in local time were prepared for all parameters.			
Nearest data				
GEOS-5	Reanalysis data produced by NASA/GMAO's GEOS-5 DAS [Rienecker et al., 2008] included Aura/MLS O ₃ and Temperature. The grid is 2.0 deg latitude x 2.5 deg longitude with 3-hour intervals; closest time and location data is used with 4-point spatial interpolation.			
SD-WACCM	CCM Simulations from SD-WACCM nudged with GEOS-5 (not including Aura/MLS). The grid is 1.9 deg latitude x 1.25 deg longitude with 0.5-hour intervals; closest time and location data on the grid is used.			
AURA/MLS	Gridded data for same day from Aura/MLS v2.2. Latitude-longitude grid is 5.0 x 5.0 degrees; closest location data is used with 4-point spatial interpolation.			

Table 2.5-2 List of a priori dataset

Data	Climatology data				Nearest data		
	Aura /MLS	UARS /MLS	CCSR /NIES	SD- WACCM	GEOS-5	SD- WACCM	Aura /MLS
O_3	•		0	0		0	
HCl	•		0	0		0	



Data	Climatolo	gy data		Nearest d	lata		
	Aura /MLS	UARS /MLS	CCSR /NIES	SD- WACCM	GEOS-5	SD- WACCM	Aura /MLS
ClO	•		0	0		0	
HNO ₃	•		0	0		0	
CH ₃ CN		0		0		•	
HOCl	0		•	0		0	
HO_2	0		•	0		0	
BrO	0		•	0		0	
Temp.	0		0	0	•	0	•
Pres.	0		0	0	•	0	
Wind			0	0	•	0	
H ₂ O	0		0	0	•	0	

^{*} o: existing data / •: data used in v2.4 processing

2.6. PRODUCT RELEASE HISTORY

We have updated our L2 product almost every six months since the launch. The following descriptions are brief summaries for each version of the L2 products. See details in Appendix A.1. Hereafter, in the 9 digit number in the description for each version "XXX-YY-ZZZZ", XXX shows the L1B data version number, YY shows that of *a priori* datasets, and ZZZZ shows that of L2 retrieval algorithms.

- v1.0 (005-06-0024): for retrieval tests (released 23/01/2010)
 V1.0 is a test processing version in order to check L2 processing algorithms designed before launch [Takahashi et al., 2010].
- v1.1 (005-06-0032): for mapping tests (released 19/04/2010)
- Pointing data was improved to increase the amount of useful data and to create gridded data.v1.2 (005-06-0150): algorithm update I (released 15/09/2010)
 - We included experimental correction factors in the AOS response function (one of the instrumental functions) which determine that retrieved temperature agrees with TIMED/SABER to suppress internal inconsistency between receivers.
- v1.3 (006-06-0200): algorithm update II (released 02/03/2011)



This version is the first update in L1B processing algorithms [For details, see level 1 Product Release Notes (Ver.006)]. Screening conditions during solar paddle interference are well defined, so abnormal values during such conditions can be properly selected.

- v2.0 (007-08-0300): major update (released 04/10/2011)
 The L1B version was updated to ver. 007 by introducing non-linearity correction. This reduced the bias of stratospheric temperature, resulting in an 8% decrease in O₃ at peak height level as well as other improvements in L2 products [*Mitsuda et al.*, 2011].
- v2.1 (007-08-0310): improvements to HOCl (released 16/01/2012)
 This was a minor update to aim to improve HOCl by re-investigating line data around HOCl. We have released this version of the data to the public (05/03/2012).
- v2.2 (007-09-0400): algorithm update
 Retrieval height range was re-investigated in order to obtain proper results in the upper
 mesosphere and the lower thermosphere, and smoothing of the retrieved profiles was taken into
 account using the Tikhonov Regularization method (TRM).
- v2.3 (007-09-0402): status flag update
 Screening conditions were re-evaluated, and the useful data rate was improved by around 30-50 %.
- v2.4 (008-11-0502): a priori profile update
 Retrieval settings were modified to improve O₃ profiles in the lower thermosphere.



3. LATEST UPDATES FOR SMILES L2 PRODUCTS

3.1. SUMMARY OF ALGORITHM UPDATES

Main improvements in the L2 algorithm after v2.1 are the three points as follows; see Appendix A.1 for details about the updates for each version.

- Extension of height range (O₃, HCl, HO₂, BrO)
 In v2.1 retrieval height range was set at 8-85 km for all parameters, but in this version the upper bound for retrieval height range is set at 120 km for O₃ and at 100 km for HCl and HO₂. At the same time a priori values and their errors are adjusted for better comparison with other data sources, resulting in improvements for those species. In addition, after adjusting a priori errors for BrO, it is possible to evaluate biases between day-time and night-time values.
- Smoothing profiles (O₃, HCl, HNO₃)
 In v2.1 some oscillations remained to the order of a few percent at 50 km for O₃ and HCl profiles, and there was divergence of HNO₃ profiles in the lower stratosphere. To reduce these erroneous behaviors we applied the Tikhonov Regularization Method (TRM) in addition to the ordinal Optimal Estimation Method (OEM) for the L2 inversion algorithm. We also use the updated AOS response function prepared by the SMILES instrument team [Mizobuchi et al., 2013]. All these improvements contribute to reducing mesospheric O₃ and HCl oscillations.
- Increase in available data
 - The number of usable profiles increases by investigating screening conditions. So far we have included quality flags for L1B data and status of L2 profile convergence, but due to field obstacle flags, about 20% of data for one of the L1B data quality flags was judged to be inappropriate for use. In addition, we looked into variations in state vectors normalized by random errors as the threshold to observe the validity of retrieval results; however, the threshold is no longer appropriate since theoretical errors become smaller after introducing the Tikhonov Regularization Method. In v2.4, as indicated in Table 3.1-1, consistency seen in HCl profiles is used for the new screening conditions. Among species that have strong line intensity such as O₃, HCl, and ClO, HCl measurements were done at all times and as its diurnal and seasonal variations are relatively small, we decided to utilize the HCl data for evaluating the quality of retrieved profiles. Moreover, we have included the fitting residual as one of the quality flags, as the residual becomes valid when using the Tikhonov Regularization Method.



Table 3.1-1 Major changes in screening flags between v2.1 and v2.4

Item	V2.1	V2.4	
Field	Field obstacle flag from L1B	Adequacy of HCl profile	
obstacles Calibration error (trouble with		Calibration error (trouble with	
	calibration mode)	calibration mode)	
Retrieval Convergence of retrieved results		Spectral residual	
results		< standard noise (0.5K)	
		Adequacy of HCl profile	

3.2. USEFUL DATA

The amounts and ratios of useful data for v2.1 and v2.4 are shown in Table 3.2-1. As mentioned in the previous section, the amount of useful data of v2.4 increases by 30 - 50 % in comparison with that of v2.1. This results in a significant improvement in the zonal mean profiles of BrO and ClO (observed in Band C), as well as in a decrease in missing points in global mapping of the data.

Table 3.2-1 Useful data differences between v2.1 and v2.4

		Number			Ratio (%)		
	A	В	С	A	В	С	
v2.1	113093	78768	69296	68.14	59.09	38.22	
v2.4	141962	112442	136036	89.39	88.78	76.29	

3.3. Profile differences between v2.4 and v2.1

$3.3.1 O_3$

SMILES observes ozone by detecting strong absorption lines at 625.37GHz with Bands A and B, and the wings of absorption lines at 647.8GHz and 650.8GHz with Band C. Band C is suitable for measuring ozone near the tropopause because there are few strong lines in the band, but as only spectrum data above 15km is considered in the present version of the retrieval process, Band C data has fewer advantages. The signal-to-noise ratio of ozone lines detected with Bands A and B is the highest among any absorption lines measured by the SMILES spectroscopy system; theoretical random error is lower than 1% at the altitude of 20 – 50 km.

The validation of O_3 data in the v2.1 product was done by comparison with satellite-borne data, CTMs (SD-WACCM and MIROC3.2-CTM) and ozonesonde data [Imai et al., 2013a, 2013b]. It was found that this data agrees within a 10% difference in stratosphere and a 30% difference in



mesosphere (see Figure 3.3-1). In addition, the diurnal components of O_3 agree well with the results of SD-WACCM and MIROC3.2-CTM. These results have been used in the analysis of diurnal variation of stratospheric and mesospheric ozone. [Sakazaki et al., 2013]

In v2.4, according to the implementation of the Tikhonov Regularization Method, averaging kernels were widened to full-width-half-maximum (which corresponds to vertical resolution) so that vibration in the retrieved profile would be suppressed. Retrieval altitude ranges have been extended and *a priori* errors have been fine-tuned, resulting in a useful altitude range extension up to 95km. In the lower mesosphere, the SMILES profile presented small peaks which were detected through other satellite observation such as SABER (see Figure 3.3-4).

Figure 3.3-3 shows the difference between v2.1 and v2.4 for profiles averaged in all latitudes and observation periods. Ozone concentration in v2.4 is a few percent higher than v2.1 at most altitudes, except for the v2.4 ozone decrease in the lower stratosphere. Such trends are common to two AOSs and all bands, which were mainly affected by revision of the AOS response function.

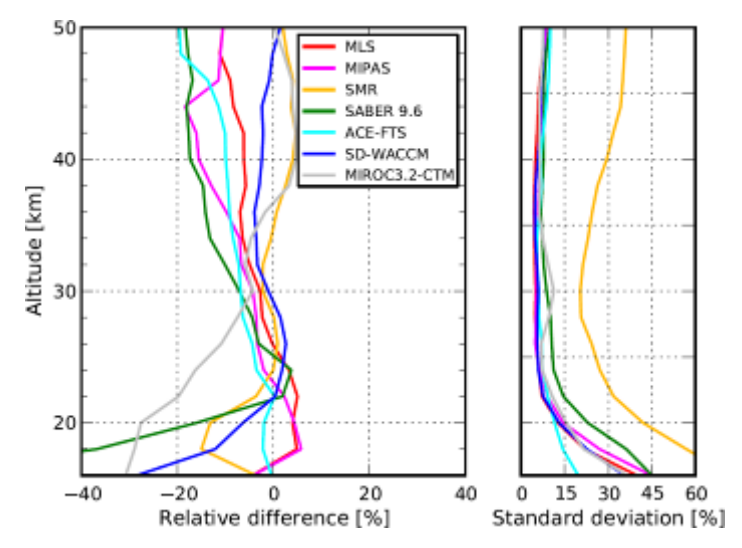


Figure 3.3-1 Relative differences ((smiles-other)/((smiles+other)*0.5)) and their standard deviations in the stratospheres. For SMILES, data from both Bands A and B are used. [*Imai et al.*, 2013a]



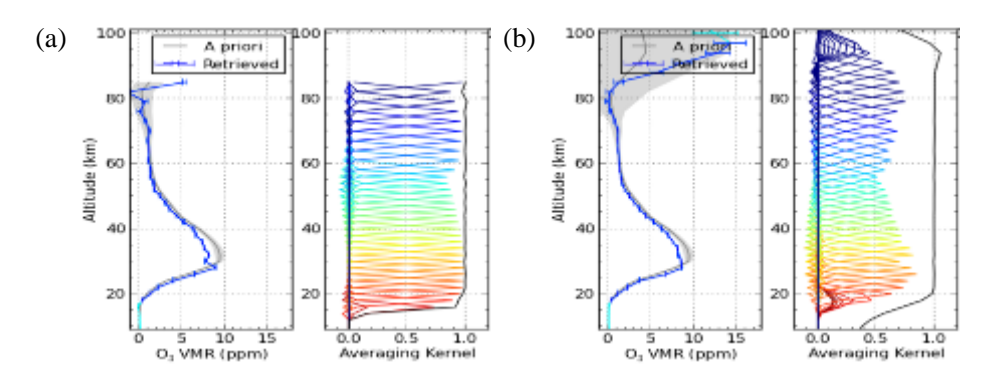


Figure 3.3-2 Sample of O_3 retrieval results at night-time near the Equator. (a) v2.1, (b) v2.4. The panels on the left show the a priori profile (gray line), errors (shaded region) and a retrieved profile (blue lines: useful altitude range, turquoise lines: un-useful altitude range). The panels on the right show averaging kernels and information values.

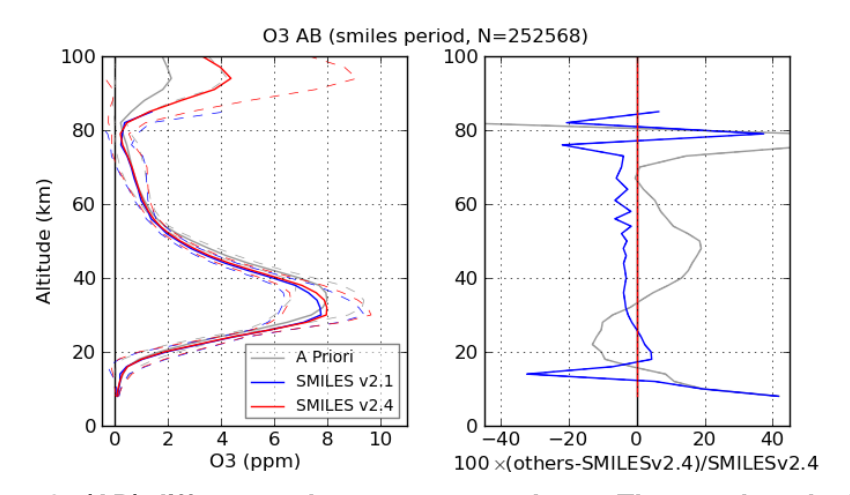


Figure 3.3-3 O_3 (AB) differences between v2.1 and v2.4. The panel on the left shows O_3 profiles averaged for all latitudes and periods. Red, blue and gray lines are v2.4, v2.1 and *a priori* profile, respectively. The panel on the right shows the relative differences between smiles v2.4 and other systems.



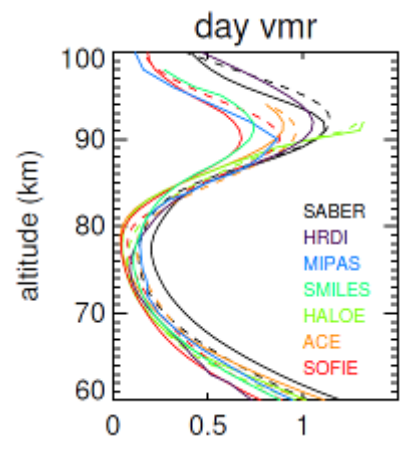


Figure 3.3-4 Averaged ozone profile for SMILES and other satellite-borne observation data (SZA < 85 deg) [*Smith et al., 2013*]

3.3.2 HCL

For HCl, SMILES detected H³⁷Cl with Band A and H³⁵Cl with Band B. Since the absorption line in Band B is stronger than that of Band A, retrieval results from Band B have better sensitivity in higher altitudes.

Improvement of v2.4 HCl included (1) profile smoothing with implementation of TRM and (2) extension of retrieval altitude range and tuning of *a priori* / *a priori* errors in the lower thermosphere, similar to the case of ozone (see Figure 3.3-5).

Figure 3.3-6 shows a comparison of averaged profiles for SMILES v2.4, v2.1 and WACCM. HCl concentration in the v2.4 profile is a few percent different from the v2.1 profile, according to the revision of the AOS response function. In v2.4 profiles, theoretical predictions, such as constant values in the mesosphere and decreases in the lower thermosphere, are present in a similar fashion to WACCM calculations.



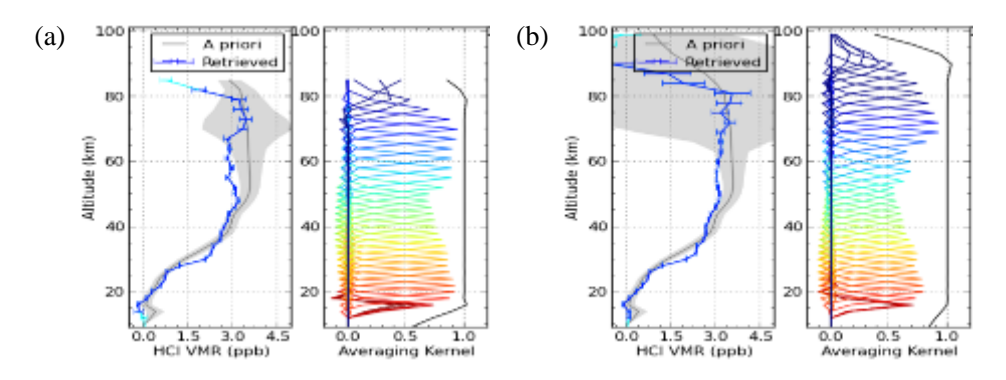


Figure 3.3-5 Sample of HCI retrieval results near the Equator. (a) v2.1, (b) v2.4, in the same format as that of Figure 3.3-2.

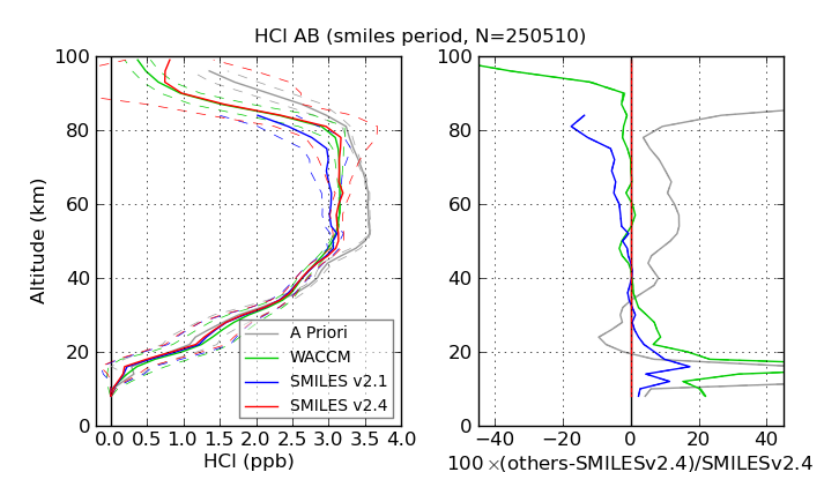


Figure 3.3-6 HCI (AB) differences between v2.1 and v2.4, in a similar format to Figure 3.3-3. The green line represents WACCM calculations.

3.3.3 CLO

CIO can be detected with the most sensitivity in Band C, so the differences in single profiles between daytime and night-time can be distinguished (see Figure 3.3-7). Suzuki et al., 2012 reported that CIO v1.2 agrees with Aura/MLS v2.2 in the stratosphere. In v1.3, CIO profiles had been compared with ground-based millimeter-wave spectrometer data, and it was reported that both were almost in agreement at an altitude of up to 40km [Kuwahara et al., 2012].

Figure 3.3-8 shows the averaging kernels of v2.4 data for daytime and night-time. According to these results, the profiles are "usable" at altitudes up to 70km for both daytime and night-time, and sensitivity is high in that altitude range. The differences in the profiles in a comparison with v2.1 data can be seen in Figure 3.3-9. It is not significant in general whether the profiles are slightly changed with the revision of AOS response function at the higher altitude and the revision of nonlinearity correction parameters at the lower altitude.



In the lower altitude region (<35 km), the SMILES CIO product shows night-time bias. The CIO value should be zero below 35 km, but it shows a bias value due to instrumental effects (Suzuki et al., 2012). This bias can be corrected by subtracting night-time zonal mean value, as already shown in the case of BrO (Stachnik et al, 2013). The bias value changes seasonally and with latitude, so it is recommended that bias value is corrected monthly with a 10° latitude bin. SMILES Acousto-Optic Spectrometer characteristics were changed after Oct. 23, 2009 when laser diode temperature levels changed.

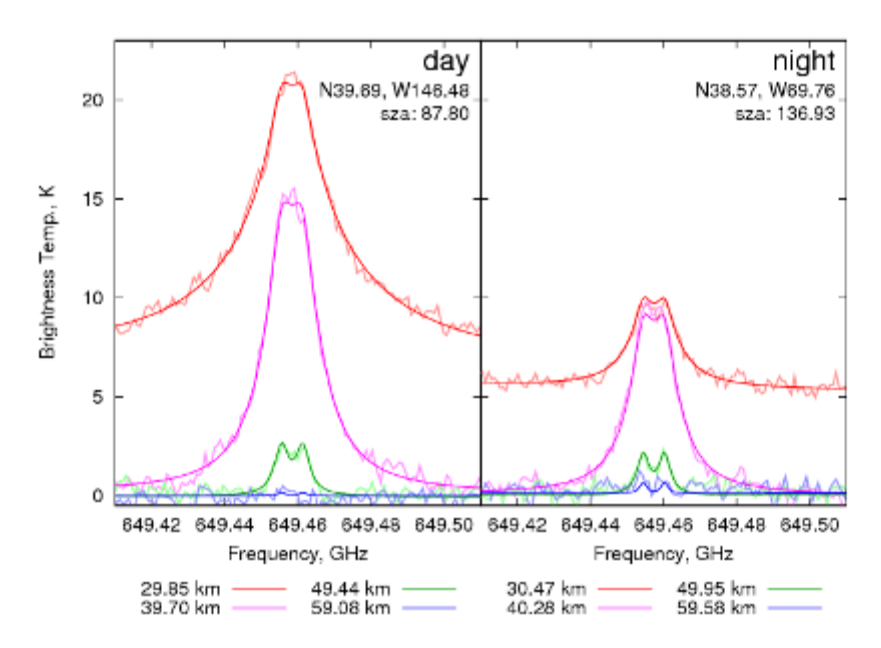


Figure 3.3-7 Examples of CIO spectra (November, middle-latitude). The thick lines show L2 spectra and the thin lines show L1B (observed) spectra. Right: day, left: night.



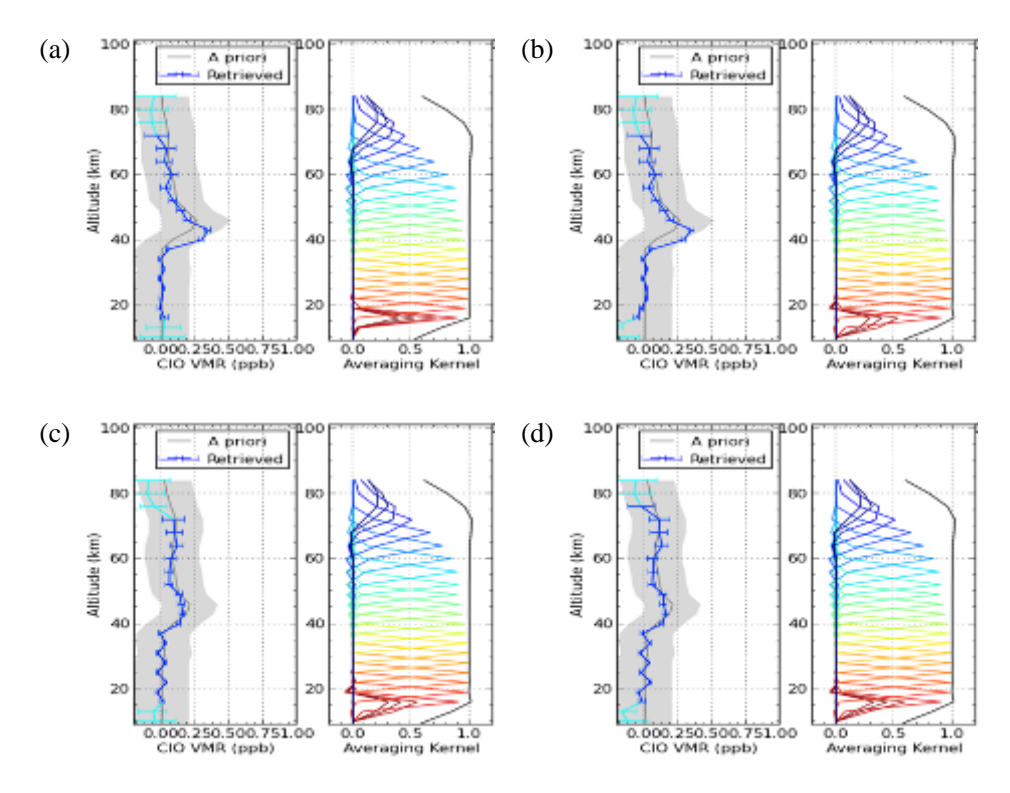


Figure 3.3-8 Sample of CIO retrieval results in northern middle-latitude. (a) v2.1, daytime, (b) v2.4 daytime, (c) v2.1, night-time, (d) v2.4, night-time, in the same format as that of Figure 3.3-2.

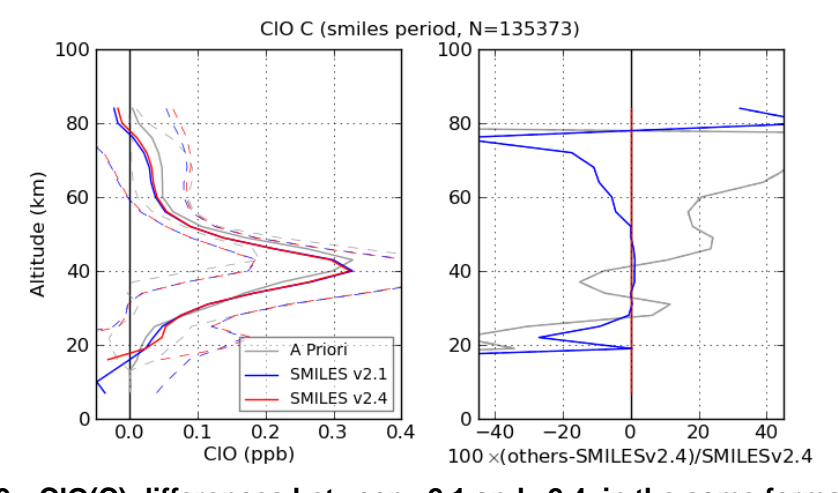


Figure 3.3-9 CIO(C) differences between v2.1 and v2.4, in the same format as that of Figure 3.3-3.

3.3.4 HNO₃

HNO₃ can be detected with Bands A and C, but there is calibration error due to the line being



positioned at the observation band in Band C, and there is some error due to the spectral wing of HCl in Band A. In order to suppress vibrations found in the lower stratosphere in the profile of v2.1 data, strong Tikhonov Regularization is implemented in v2.4 data processing (see Figure 3.3-10) [Manago et al., 2013]. In addition, the peak value of the profile from Band A data has been decreased so that the profile from Band A data is closer to that of Band C data (see Figure 3.3-11).

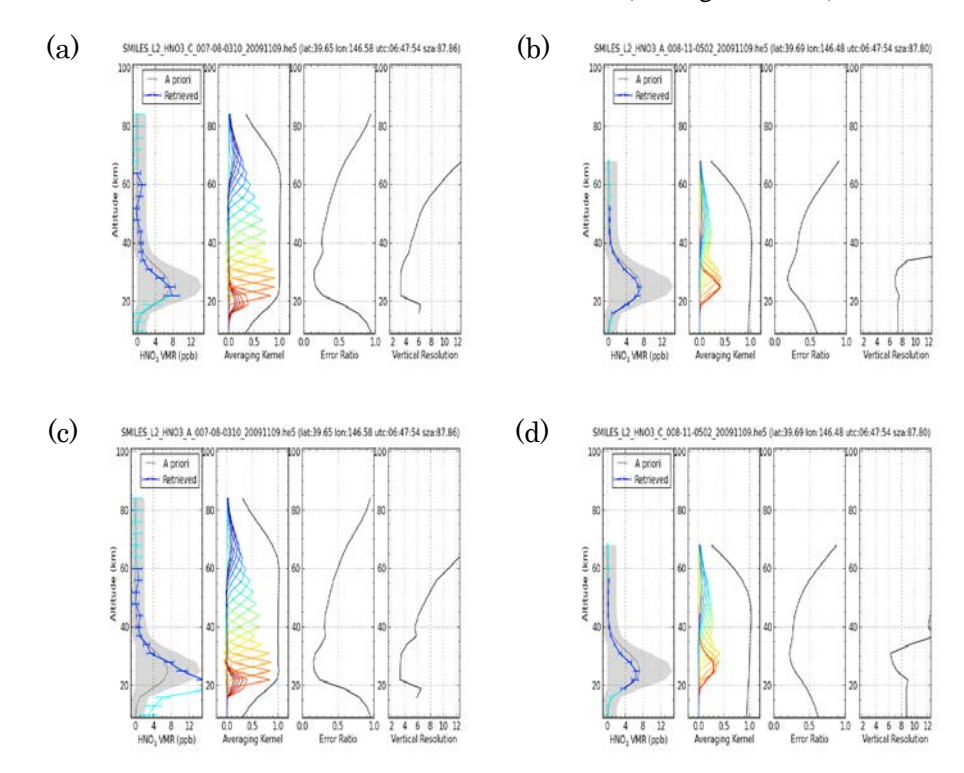


Figure 3.3-10 Sample of HNO_3 retrieval results in northern middle-latitude. (a) v2.1, Band C, (b) v2.4, Band C, (c) v2.1, Band A, (d) v2.4, Band A, in the same format as that of Figure 3.3-2.



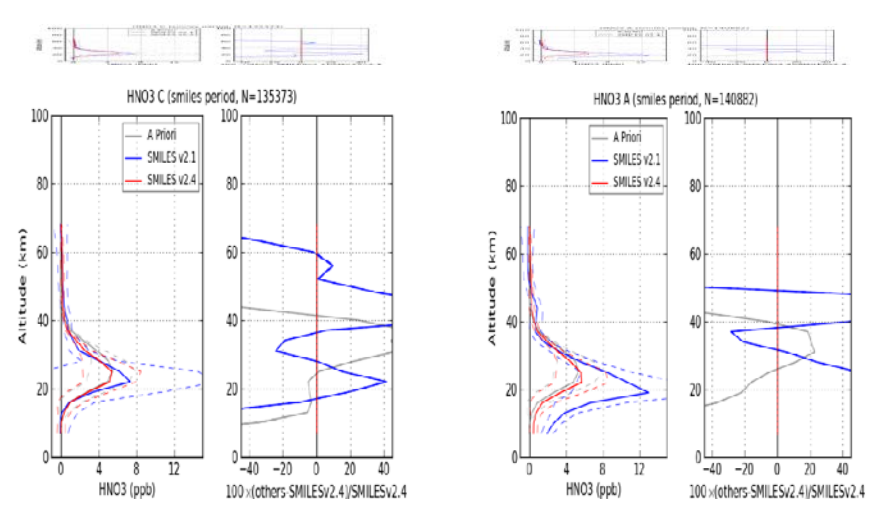


Figure 3.3-11 HNO_3 (C, A) differences between v2.1 and v2.4, in the same format as that of the panel on the left in Figure 3.3-2.

3.3.5 HOCL

HOCl can be detected with Band A, but its spectral line is positioned at the shoulder of excited O_3 and O_3 isotopes, so HOCl retrieval is affected by O_3 line parameter and calibration errors in the lower stratosphere. In order to suppress vibrations in the HOCl profile, a smoothing process with altitude correlation has been implemented since v2.0 retrieval, but the *a priori* profile which comes from climatological Aura/MLS data has some vibrations in v2.1, so these profiles were reflected in the retrieval results. In the v2.4 retrieval process, CCSR/NIES climatological data is adopted as *a priori* profiles instead of Aura/MLS data, so that some "sub-peaks" at around 30km have been suppressed (see Figure 3.3-13).

In averaged profiles, the amount at higher than 40km slightly increases in comparison to v2.1 data, and negative values at around 50km for daytime profiles have been eliminated. On the other hand, some vibrations still remain at lower than 40km in the profiles, so further improvement seems to be necessary (see Figure 3.3-14).



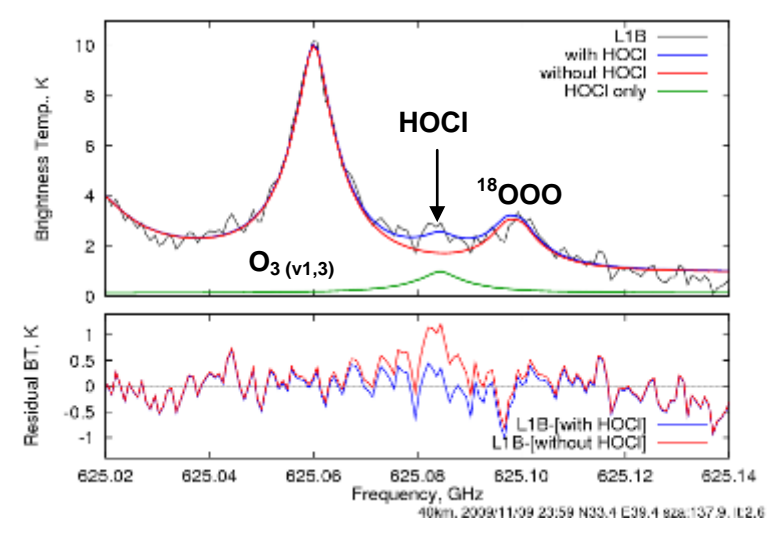


Figure 3.3-12 Example of HOCI Spectrum at 40km

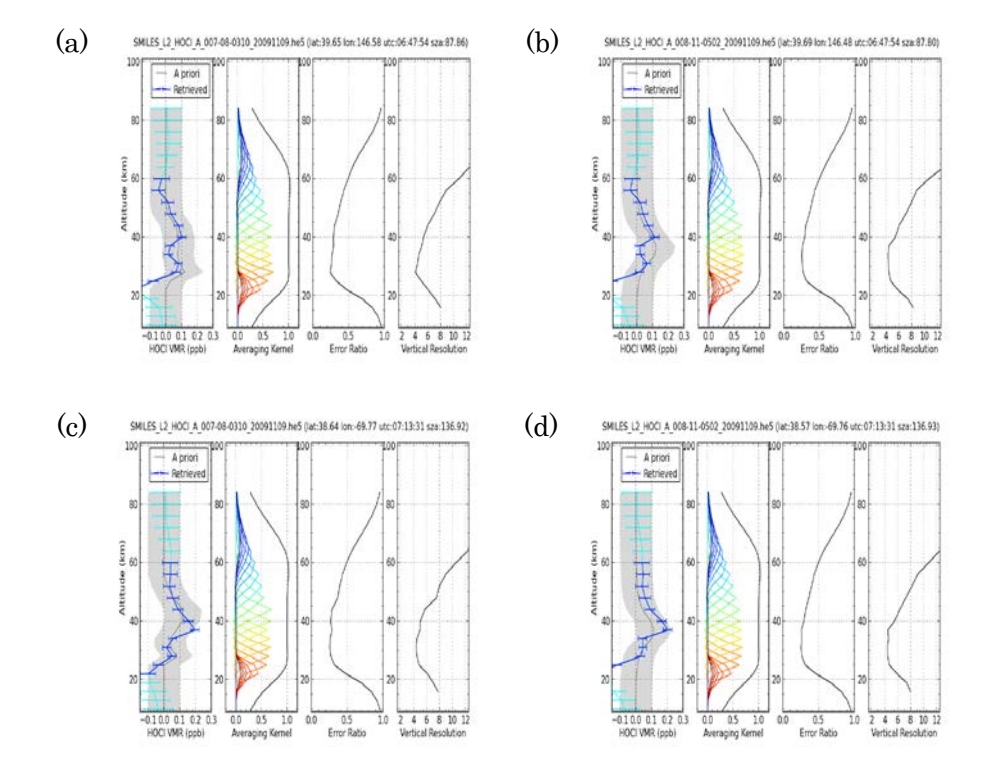


Figure 3.3-13 Sample of HOCI retrieval results in northern middle-latitude. (a) v2.1, daytime, (b) v2.4 daytime, (c) v2.1, night-time, (d) v2.4, night-time, in the same format as that of Figure 3.3-2



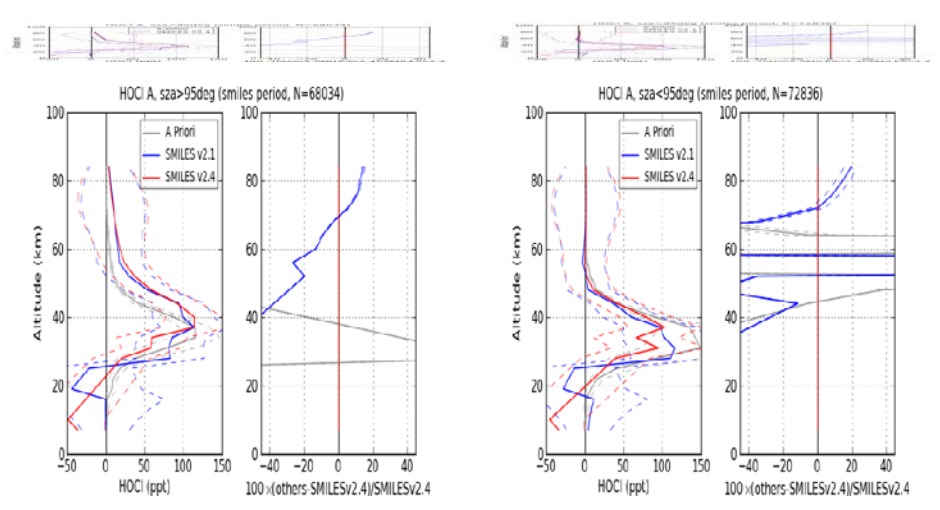


Figure 3.3-14 HOCI (night-time, daytime) differences between v2.1 and v2.4, in the same format as that of the panel on the left in Figure 3.3-2.

3.3.6 CH₃CN

CH₃CN can be detected only with Band A, but its retrieval is affected by the spectral wing of HCl lines. In v2.1 retrieval, UARS/MLS climatological data*, which is discontinuous at an altitude of around 20km, was referred to for the *a priori* profile. In order to eliminate the effect of the discontinuous profiles, the nearest grid data of SD-WACCM calculations is adopted as an *a priori* value (see Figure 3.3-15). There is little difference above 25km in comparison to v2.1 profiles. (* Constant 0.15ppb is adopted at lower than 15km according to ground-based results, and 15 – 20km is treated as a transition zone)

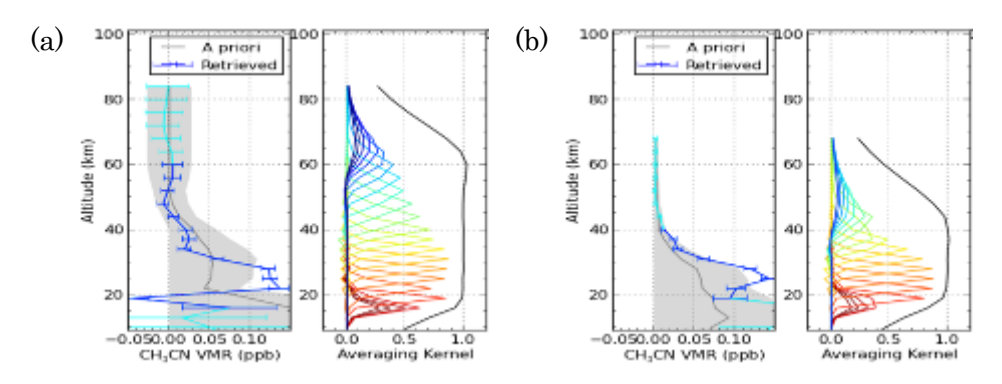


Figure 3.3-15 CH₃CN(A) differences between v2.1 and v2.4, in the same format as that of Figure 3.3-3





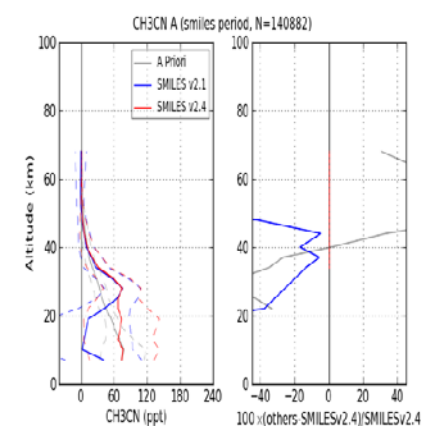


Figure 3.3-16 CH3CN differences between v2.1 and v2.4, in the same format as that of the panel on the left in Figure 3.3-2.

3.3.7 BRO

BrO can be detected with Bands A and C. While the BrO line is overlapping with other spectral lines, the ozone isotope line that overlaps with the BrO line in Band C is more intense and the ozone isotope can retrieve other lines of different frequencies, so it is recommended that BrO results from Band C are used.

In comparison to v2.1 retrieval, a priori and its error values (lower limit) have been modified in v2.4 retrieval. As a result, stratospheric BrO can be retrieved at night-time (see Figure 3.3-18). According to calculations with numerical chemical models, stratospheric BrO will approach zero at night-time, so BrO amounts retrieved can be acknowledged to have some bias. Considering this bias, BrO amounts obtained in v2.3 retrieval would be consistent with the *in situ* balloon experiment [*Stachnik et al.*, 2013]. Biased data will be delivered in addition to data products themselves.

In v2.4 products, the BrO amount has decreased (*i.e.* negative bias) at a lower altitude caused by non-linearity correction. In addition, standard deviation of daytime BrO has also decreased because of the suppression of vibrations in HNO₃ profiles (see Figure 3.3-19).

Similar to the case of ClO, the BrO product shows night-time bias. The BrO value should be zero below 35 km. This bias can be corrected by subtracting night-time zonal mean value, as already shown in the case of BrO. [Stachnik et al., 2013] The bias value changes seasonally and with latitude, so it is recommended that bias value is corrected monthly with a 10° latitude bin. SMILES Acousto-Optic Spectrometers' characteristics were changed after Oct. 23, 2009 when laser diode temperature levels changed.



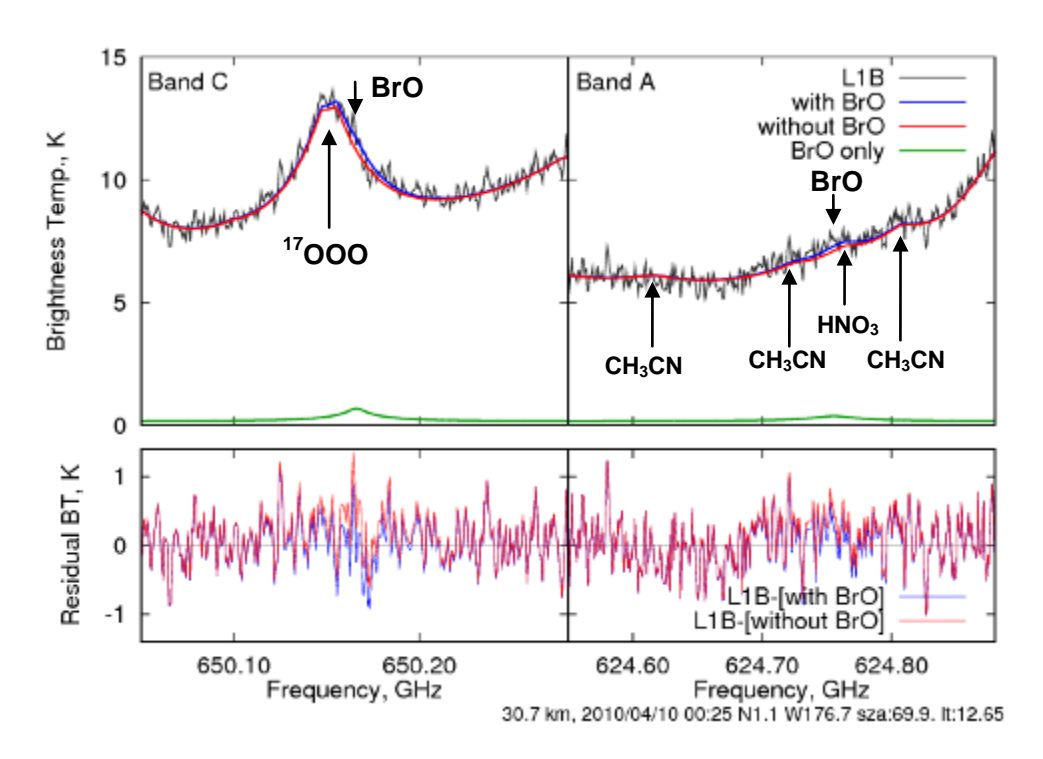


Figure 3.3-17 Examples of BrO spectrum at 30 km



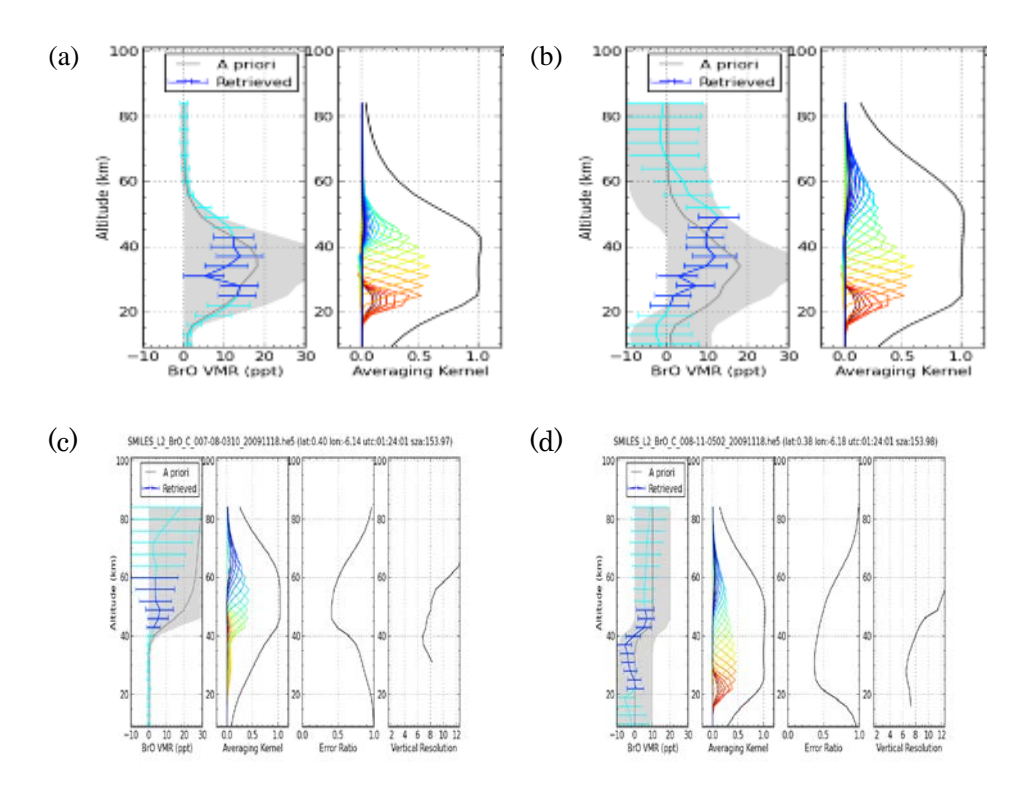


Figure 3.3-18 Sample of BrO (C) retrieval results near the Equator. (a) v2.1, daytime, (b) v2.4 daytime, (c) v2.1, night-time, (d) v2.4, night-time, in the same format as that of Figure 3.3-2

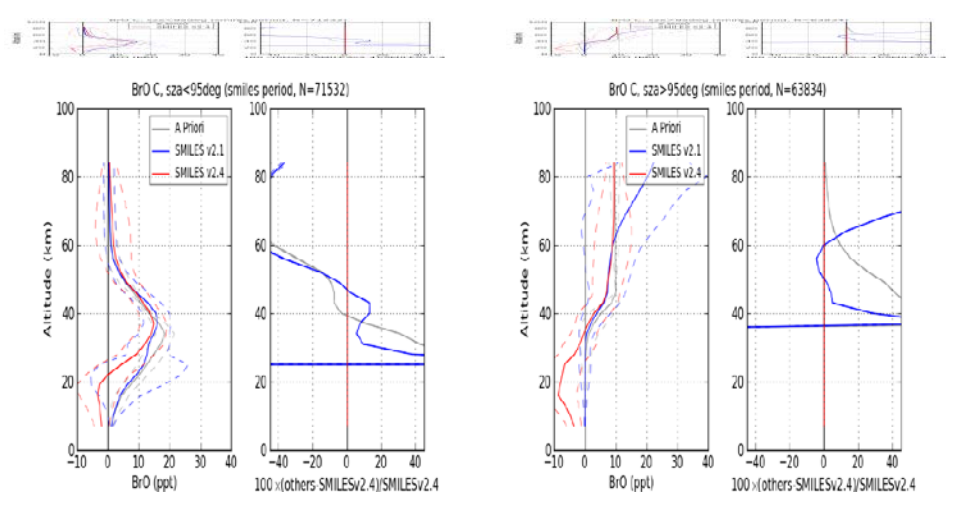


Figure 3.3-19 BrO (night-time, daytime) differences between v2.1 and v2.4, in the same format as that of the panel on the left in Figure 3.3-2.

3.3.8 HO₂

HO₂ can be detected with Bands B and C, and there are independent spectral lines with comparable intensity in both bands. It was impossible to obtain mesospheric HO₂ at night-time with



v2.1 retrieval because of the small values of *a priori* errors. In v2.4 retrieval, a priori errors have been extended, so that HO₂ can be retrieved up to an altitude of 90km. As a result, there was a peak of around 80km in the profiles which had not been recognized with older versions of the product (see Figures 3.3-21 and 3.3-22). However, stratospheric values in HO2 profiles still have different biases in each band and these will be re-evaluated in further studies in a similar manner to BrO profiles.

Similar to the cases of ClO and BrO, HO₂ value should be zero below 35 km at night-time. However, it shows bias value due to instrumental effects.[Suzuki et al., 2012] This bias can be corrected by subtracting night-time zonal mean value, as already shown in the case of BrO. [Stachnik et al., 2013] The bias value changes seasonally and with latitude, so it is recommended that bias value is corrected monthly with a 10° latitude bin. SMILES Acousto-Optic Spectrometers' characteristics were changed after Oct. 23, 2009 when laser diode temperature levels changed.

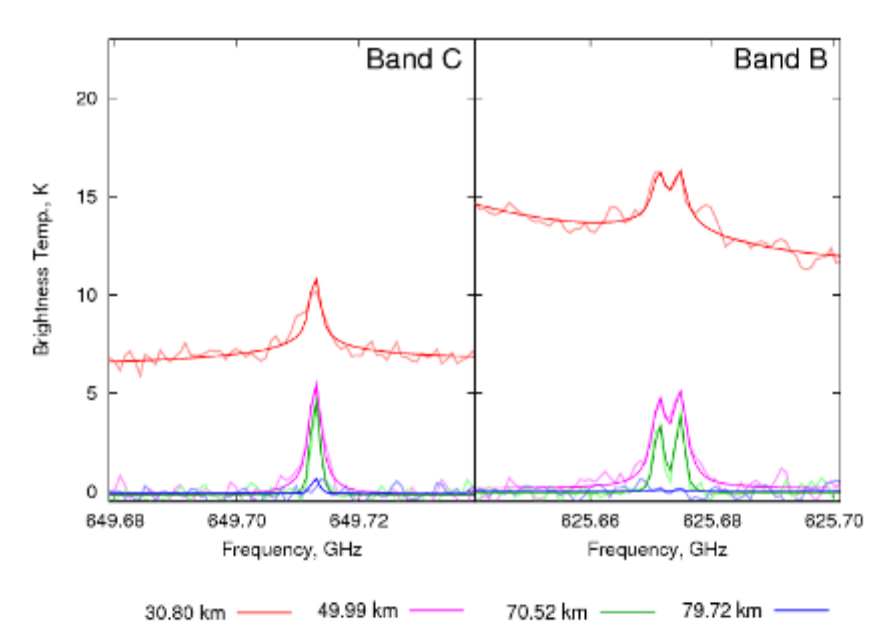


Figure 3.3-20 Examples of HO₂ Spectra (November, near Equator). Thick lines show L2 spectra and thin lines show L1B (observed) spectra. left) Band C, right) Band B.



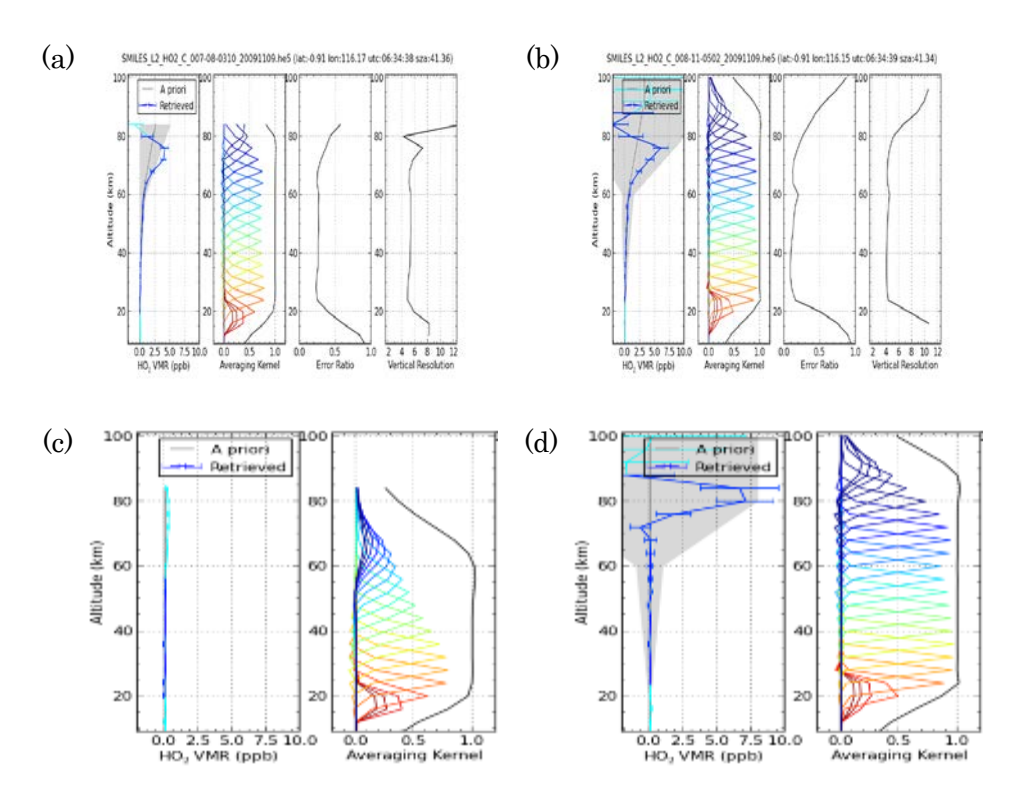


Figure 3.3-21 Sample of HO_2 (C) retrieval results near the Equator. (a) v2.1, daytime, (b) v2.4 daytime, (c) v2.1, night-time, (d) v2.4, night-time, in the same format as that of Figure 3.3-2

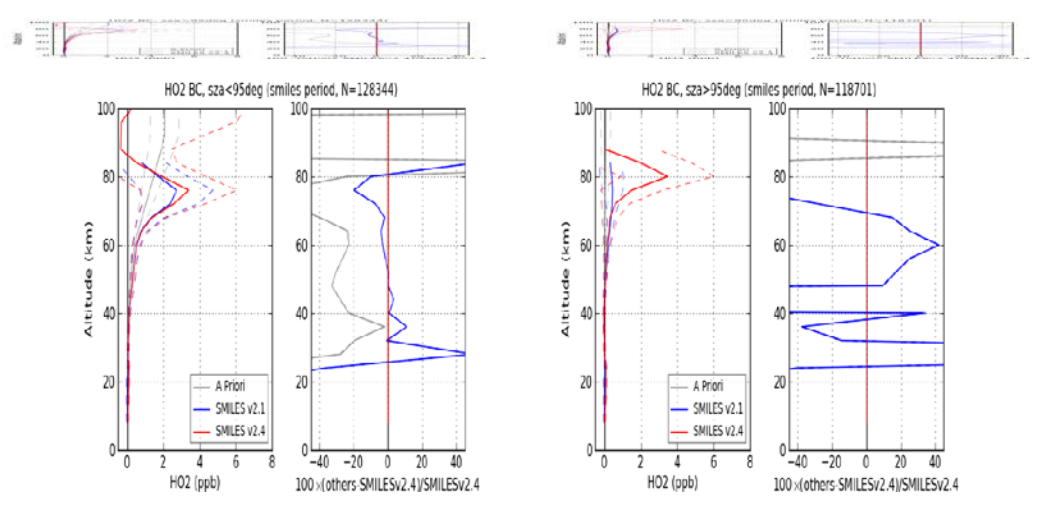


Figure 3.3-22 HO₂ (night-time, daytime) differences between v2.1 and v2.4, in the same format as that of the panel on the left in Figure 3.3-2

3.3.9 TEMPERATURE

There is no measurable spectral line of O_2 in the SMILES observation bands, so temperature profiles are retrieved with O_3 and HCl lines in Bands A and B. Since the v2.1 algorithm, *a priori* data with



small errors has been directly referred in the retrieval process in order to avoid errors with retrieving mesospheric temperature. The V2.4 algorithm follows the principle adopted in v2.1 (see. Figure 3.3-23). However, using the nearest grid of Aura/MLS climatological data to impose some tidal effects with GSWM data as *a priori* values has resulted in enhanced vibration in HCl profiles in tropical regions. In order to resolve this problem in the v2.4 algorithm, GEOS-5 data which is nudged with Aura/MLS temperature and O₃ data up to the mesosphere has been adopted up to 60km, and tidal effects have been calculated within GEOS-5 data. For altitudes higher than 60km, the nearest grid in Aura/MLS climatology data is directly referred to as *a priori*.

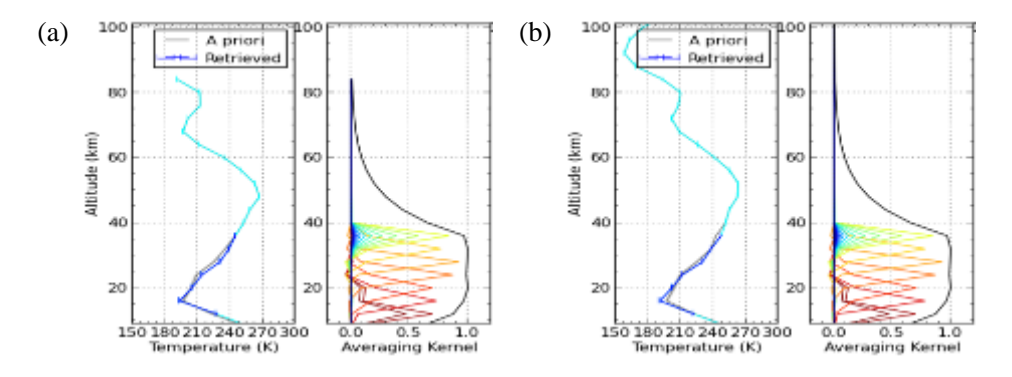


Figure 3.3-23 Sample of temperature retrieval results near the Equator. (a) v2.1, (b) v2.4, in the same format as that of Figure 3.3-2.

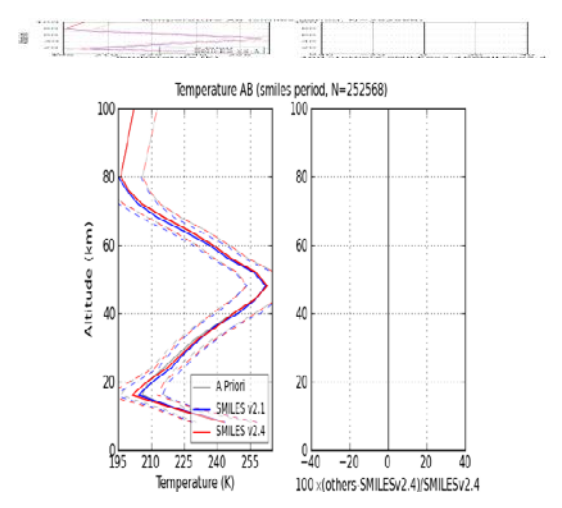


Figure 3.3-24 Temperature differences between v2.1 and v2.4, in the same format as that of the panel on the left in Figure 3.3-2.

$3.3.10 O_3$ ISOTOPES

SMILES can detect 3 out of 4 types of O₃ isotope excluding O¹⁸OO. ¹⁸OOO and ¹⁷OOO in Band C are relatively easy to retrieve because their spectral lines are positioned independently with other



lines, but ¹⁸OOO and O¹⁷OO in Band B are positioned at the shoulder of the intense spectral lines of O₃ and HCl respectively, so retrieval results of those isotopes are likely to be affected by O₃ and HCl results. In v2.4 retrieval algorithms, lower limit values of a priori O₃ isotopes have been modified, which resulted in an extension of their sensitive altitude range (see Figures 3.3-25, 3-3.26, and 3.3-27). Averaged profiles differ by a few percent at the peak altitude and by around 5% in the mesosphere caused by the revision of AOS response function and that of non-linear correction. In addition, ¹⁸OOO (Band B) differed by around -10% at the peak altitude according to the revision of spectral line parameter (see Figure 3.3-28).

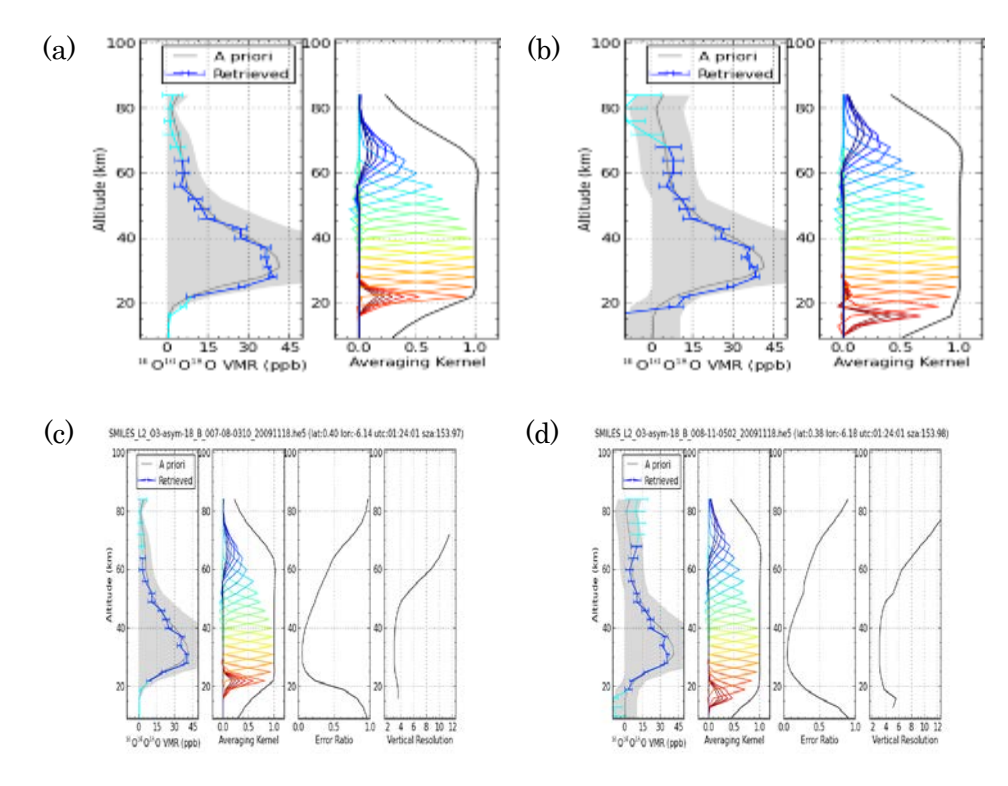


Figure 3.3-25 Sample of 18 OOO retrieval results near the Equator . (a) v2.1, Band C, (b) v2.4, Band C, (c) v2.1, Band B, (d) v2.4, Band B, in the same format as that of Figure 3.3-2.



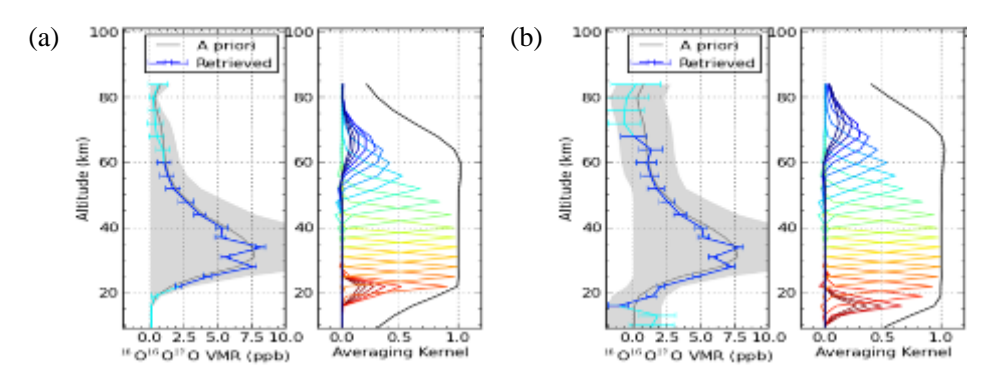


Figure 3.3-26 Sample of 17 OOO retrieval results near the Equator . (a) v2.1, (b) v2.4., in the same format as that of Figure 3.3-2.

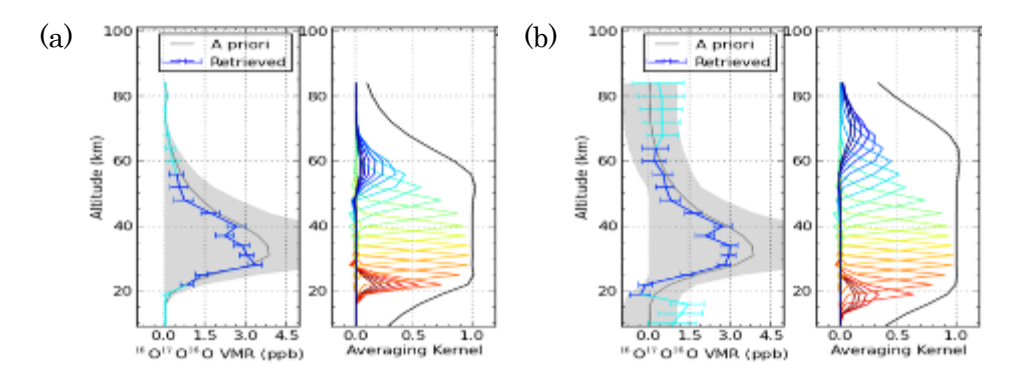


Figure 3.3-27 Sample of $O^{17}OO$ retrieval results near the Equator . (a) v2.1, (b) v2.4, in the same format as that of Figure 3.3-2.



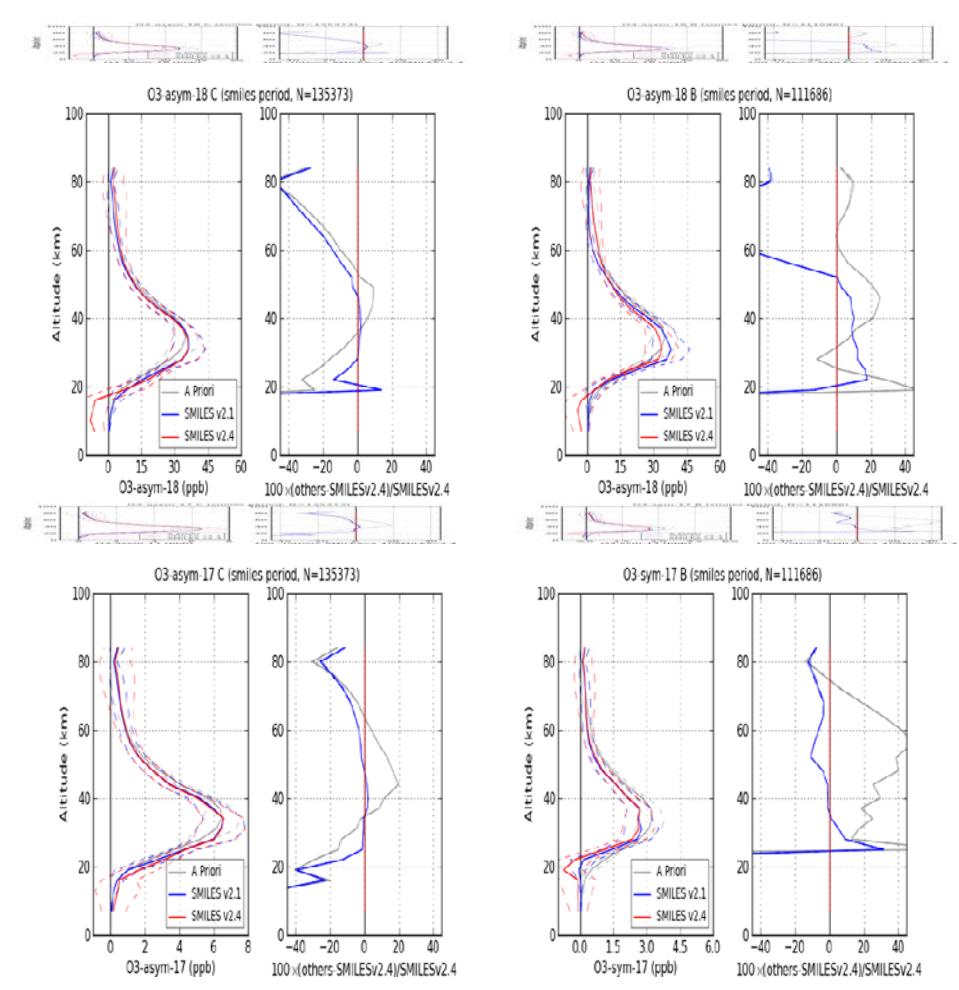


Figure 3.3-28 O3 Isotioes differences between v2.1 and v2.4, in the same format as that of the panel on the left in Figure 3.3-2.

3.4. REMAINING ISSUES

- The Dicke narrowing effect was not considered and the profiles in the upper mesosphere may have negative bias. However, we have found that this effect is small in reality.
- Frequency calibration in L1 processing has long-term drift.
- Differences between profiles retrieved from AOS1 and AOS2 according to the revision of AOS
 response function. For O₃ and HCl in Band A, those differences are as high as around 5% in the
 mesosphere.



4. SMILES L2 PRODUCTS

4.1. DEFINITION OF DATA PRODUCTS

The definitions of datasets are in Table 3.1-1. The DPS-L2 produces Level 2 data to convert the calibrated measurements of brightness temperature called Level 1B data into vertical distributions of geophysical parameters along the measurement track of the instrument. The main geophysical parameters retrieved are in Table 3.1-2

Table 3.1-1 SMILES Datasets

Data type	Description
RAW	Unprocessed mission data in binary packets
Level 0	Reconstructed, unprocessed mission data in binary packets
Level 1B	Calibrated instrument radiances and related data
Level 2	Derived geophysical variables at the same resolution and location as Level 1 source data
Level 3	Variables mapped on uniform space-time grid scales, usually with some
(at a glance)	completeness and consistency

4.2. L2 PRODUCTS OVERVIEW

There are two types of SMILES L2 products. One is "L2Product" and the other is "L2Product_G_RA". The file names are defined as follows.

L2Product_G_RA:

SMILES_L2_{product_name}_{version_name}_{observed_date}.he5

L2Product:

SMILES_L2_{product_name}_{band_name}_{version_name}_{observed_date}.he5

"L2Product" includes all available datasets retrieved from all observation bands. Each file is separately provided by species, observed date and observation band. Data fields include priori profiles, averaging kernels and retrieved profiles of the pressure grid (see Table 4.4 2). As a result,



the size of each file is up to 8MB.

For "L2Product_G_RA", each file is separately provided by species and observed date. For profiles retrieved with multiple bands, only the data from the band with higher "band priority" is provided. Data fields include only 5 items. As a result, the size of each file has been reduced to 0.8MB.

Product Priority Product Priority Priority Product O_3 A, B(, C)HC1 ClO C B, A HNO₃ C(, A)HOC1 A CH₃CN A BrO HO_2 B, C A, B C(, A)Temperature

В

¹⁸OOO

B, C

 $O^{17}OO$

 \mathbf{C}

Table 4.2-1: Band priorities for each product

4.3. DATA SCREENING

17**000**

This version of the L2 product includes all the processed profiles but some of these are inadequate for scientific use. If using these profiles, we strongly recommend that usable scans are selected according to the following screening condition: status = 0 (for details, see Table 4.4-2). Moreover, L2 products include data for altitude range that is not usable for validation and/or scientific purposes. If retrieval errors that include spectrum data information are not sufficiently smaller than errors without spectrum data, L2 profiles will be retrieved from other information (such as *a priori* profiles, smoothing effects of Tikhonov Regularization). In that case, these profiles should not be used in scientific analysis. In v2.4 algorithms, the threshold of effectiveness is set to 50%, and if retrieval errors exceed the threshold, the data in L2Precision field transforms into a negative value in order to notify data users.

4.4. PRODUCT FORMAT

We show the format of the HDF-EOS5 data file below.



Table 4.4-1 Structure of HDF-EOS5 data file

No.	Group	Attributes
1	HDFEOS	Observation and retrieved data using retrieved
	/SWATH	altitude grids
	/{product_name}	Retrieved profile
		Status flag
		Geolocation data and so on
2	HDFEOS	Observation and retrieved data interpolated
	/SWATH	pressure grids
	/{product_name}_Pressure	
3	HDFEOS/	File information such as:
	ADDITIONAL/	Instrument Name
	FileAttribute	• Processing Level
		• Version
		Observation Day
		Band Name and so on

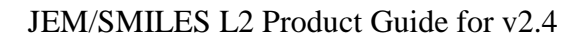
^{*:} http://www.hdfgroup.org/

(1) Standard processing data (HDF5-EOS)

The structure of standard processing data is as follows.

Table 4.4-2 : Detailed structure of L2 product files (Underlined fields are included in both types of L2 Product files)

Gr	Group/Dataset name			Explanation	Dimension	Type	Unit
<u>H</u>	DFE	<u>os</u>					
	<u>SW</u> A	4TF	<u>I</u>				
	<u>{</u>	Pro	ductname]*1				
		D	ata Fields				
			L2Value*2	Retrieved Value	(nLevel,nTimes)	float	vmr
			L2Precision	Calculation Error (negative values show unuseful data)	(nLevel,nTimes)	float	vmr
			PrecisionWOsignal	Calculation Error without Signal Information	(nLevel,nTimes)	float	vmr
			MeasurementError	Measurement Error	(nLevel,nTimes)	float	vmr
			SmoothingError	Smoothing Error	(nLevel,nTimes)	float	vmr





Group	p/Dataset name	Explanation	Dimension	Type	Unit
	Apriori	A Priori Value	(nLevel,nTimes)	float	vmr
	AprioriError	A Priori Error	(nLevel,nTimes)	float	vmr
	CorrLength	Correlative Length of A Priori	(nTimes)	float	km
	AveragingKernel	Averaging Kernel	(nLevel,nLeveln Times)	float	-
	VerticalResolution	Vertical Resolution	(nLevel,nTimes)	float	km
	Information Value	Information Value	(nLevel,nTimes)	float	-
	<u>Pressure</u>	Retrieved Pressure	(nLevel,nTimes)	float	hPa
	AprioriPressue (Temperature product only)	A Priori Pressure	(nLevel,nTimes)	float	hPa
	<u>Temperature</u> (Except Temperature product)	Retrieved Temperature	(nLevel,nTimes)	float	K
	WaterVapor	Using Water Vapor of Retrieval	(nLevel,nTimes)	float	vmr
	Baseline0	Coefficient of Continuum	(nLevel,nTimes)	float	km ⁻¹
	Baseline0Precision	Baseline Error of Coefficient	(nLevel,nTimes)	float	km ⁻¹
	Baseline1	Primary Coefficient of Continuum	(nLevel,nTimes)	float	Hz ⁻¹ .km ⁻¹
	Baseline1Precision	Baseline Error of Primary Coefficient.	(nLevel,nTimes)	float	Hz ⁻¹ .km ⁻¹
	Baseline2	2nd Coefficient of Continuum	(nLevel,nTimes)	float	Hz ⁻² .km ⁻¹
	Baseline2Precision	Baseline Error of 2nd Coefficient	(nLevel,nTimes)	float	Hz ⁻² .km ⁻¹
	Baseline3	3rd Coefficient of Continuum	(nLevel,nTimes)	float	Hz ⁻³ .km ⁻¹
	Baseline3Precision	Baseline Error of 3rd Coefficient	(nLevel,nTimes)	float	Hz ⁻³ .km ⁻¹
	RadianceResidualMax	Max. Radiance Residual	(nTimes)	float	K
	RadianceResidualMean	Mean Radiance Residual	(nTimes)	float	K
	RadianceResidualRMS	RMS Radiance Residual	(nTimes)	float	K
	RetrievedViewAngleOffset	Antenna Elevation Angle Offset	(nTimes)	float	degrees
	RetrievedViewAngleOffsetError	Antenna Elevation Angle Offset Error	(nTimes)	float	degrees
	NumIterPerform	Convergence Loop Number and Result	(nTimes)	int	-
	MaxNumIteration	Max. Convergence Number	(nTimes)	int	-
	<u>Status</u>	Status Information Useful Data = 0 Frror Status Spectrum Fitting = 1 Altitude Range = 2 Convergence Status = 4 HCl Profile Status = 8	(nTimes)	int	-
	SeqCount	Sequence Counter	(nTimes)	int	-
	AOSUnitNum	Number of Observed AOS Unit	(nTimes)	int	-
	Convergence	Convergence Status	(nTimes)	float	-



oup/	Dataset name	Explanation	Dimension	Type	Unit
	FOVInterference	Interference Flag NO Interference = 0 Interference by Sun = 1 / Moon = 2 / Solar Paddle = 4 NO information = -1	(nTimes)	int	
	CostfunctionYAll	Cost/function of Spectra	(nTimes)	float	
	CostfunctionY	Cost/function of Spectra for each Altitude	(nLevel,nTimes)	float	
	DifferenceYAll	Maximum HCl Difference between Scan and Zonal Mean Profile normalized by std.	(nTimes)	float	
	DifferenceY	HCl Difference between Scan and Zonal Mean Profile normalized by std.	(nLevel,nTimes)	float	
	Geolocation Fields	· ·			
	<u>Time</u>	Observation Time (Total no. of seconds since 1/1/1958)	(nTimes)	double	secon
	<u>TimeUTC</u>	Observation Time (UTC) yyyy-mm-dd hh:mm:ss.sss	(nTimes)	char	
	<u>Altitude</u>	Representative Altitude	(nLevel)	float	k
	<u>Latitude</u>	Observation Latitude	(nTimes)	float	degre
	<u>Longitude</u>	Observation Longitude	(nTimes)	float	degre
	<u>SolarZenithAngle</u>	Solar Zenith Angle	(nTimes)	float	degre
	<u>LocalTime</u>	Local Time	(nTimes)	float	
	<u>LineOfSightAngle</u>	Azimuth View	(nTimes)	float	degre
	AscendingDescending	Ascending/Descending Flag (Asc = 0 / Desc = 1)	(nTimes)	char	
	Reserved	Reserved Field	(nTimes)	int	
{/	Productname}_Pressure*3				
	Data Fields				
	L2Value	Retrieved Value	(nLevel,nTimes)	float	V
	L2Precision	Calculation Error	(nLevel,nTimes)	float	V
	RadianceResidualMax	Max. Radiance Residual	(nTimes)	float	
	RadianceResidualMean	Mean Radiance Residual	(nTimes)	float	
	RadianceResidualRMS	RMS Radiance Residual	(nTimes)	float	
	NumIterPerform	Convergence Loop Number and Results	(nTimes)	int	
	Status	Status Information • Useful Data = 0 • Error Status Spectrum Fitting =1 Altitude Range =2 Convergence Status = 4 HCl Profile Status = 8	(nTimes)	int	
	SeqCount	Sequence Counter	(nTimes)	int	
	AOSUnitNum	Number of Observed AOS Units	(nTimes)	int	



Group	p/Dataset name	Explanation	Dimension	Туре	Unit
	Convergence	Convergence Status	(nTimes)	float	-
	FOVInterference	Interference Flag No Interference = 0 Interference by Sun = 1 / Moon = 2 / Solar Paddle = 4 No Information = -1	(nTimes)	int	-
	CostfunctionYAll	Cost/function of Spectra	(nTimes)	float	-
	DifferenceYAll	Maximum HCl Difference between this Scan and Zonal Mean Profile normalized by std.	(nTimes)	float	-
	Geolocation Fields				
	Time	Observation Time (Total no. of seconds since 1/1/1958)	(nTimes)	double	seconds
	TimeUTC	Observation Time (UTC) yyyy-mm-dd hh:mm:ss.sss	(nTimes)	char	-
	Pressure	Representative Pressure	(nLevel)	float	hPa
	Latitude	Observation Latitude	(nTimes)	float	degrees
	Longitude	Observation Longitude	(nTimes)	float	degrees
	SolarZenithAngle	Solar Zenith Angle	(nTimes)	float	degrees
	LocalTime	Local Time	(nTimes)	float	-
	LineOfSightAngle	Azimuth View	(nTimes)	float	degrees
	AscendingDescending	Ascending/Descending Flag (Asc = 0 / Desc = 1)	(nTimes)	char	-
	Reserved	Reserved Field	(nTimes)	int	-
	ADDITIONAL				
	FILE_ATTRIBUTES*4				
HDF	FEOS INFORMATION				
<u>Str</u>	ructMetadata.0	Matrix Information for Swath Data	1	char	-
<u>co</u> .	remetadata.0	HDF-EOS Information	1	char	-

^{*1} Attributes of {Productname} group

No.	Name	Explanation	Dimension	Data type	Unit
1	Altitude	Calculation Altitude	(nLevels)	float	km
2	VerticalCoordinate	Vertical Coordinate System Name	-	char	

^{**2} Attributes of Dataset in Geolocation/Data fields group



No.	Name	Explanation	Dimension	Data type
1	Missing Value	Missing Value	-	float
2	Title	File name	-	char
3	Units	Unit	-	char
4	UniqueFieldDefinition	Field Definition	-	char

**3 Attributes of {Productname}_pressure group

No.	Name	Explanation	Dimension	Data type	Unit
1	Pressure	Calculation Pressure	(nLevels)	float	hPa
2	VerticalCoordinate	Vertical Coordinate System Name	-	char	

**4 Attributes included File Attribute group

No.	Name	Explanation	Dimension	Data type
1	L1BID	L1B File Name	(nTimes)	char
2	InstrumentName	Instrument Name (SMILES)	-	char
3	ProcessLevel	Processing Level (L2)	-	char
4	StartUTC	Start Time for File (yyyy-mm-ddT00:00:00.000)	-	char
5	EndUTC	End Time for File (yyyy-mm-dd T23:59:59.000)	-	char
6	GranuleMonth	Month (mm)	-	int
7	GranuleDay	Day (dd)	-	int
8	GranuleDayofYear	Granule Day of Year	-	int
9	Granule Year	Year (yyyy)	-	int
10	PGEVersion	Processing Version (XXX-XX-XXXX)	-	char
11	StartScan	Scan Count for First Day for File	-	char
12	EndScan	Scan Count for End Day for File	-	char
13	BandName	Band Name	-	char



REFERENCES

- Akiyoshi, H., L. B. Zhou, Y. Yamashita, K. Sakamoto, M. Yoshiki, T. Nagashima, M. Takahashi, J. Kurokawa, M. Takigawa, and T. Imamura (2009), A CCM simulation of the breakup of the Antarctic polar vortex in the years 1980-2004 under the CCMVal scenarios, *J. Geophys. Res.*, 114, D03103, doi:10.1029/2007JD009261.
- Akiyoshi H., Yamashita Y., Sakamoto.K, Zhou.L.B., and Imamura T. (2010), Recovery of stratospheric ozone in calculations by the Center for Climate System Research/National Institute for Environmental Studies chemistry-climate model under the CCMVal-REF2 scenario and a no-climate-change run. *J.Geophys.Res.*, 115, D19301.
- Froidevaux, L., Y. B. Jiang, A. Lambert, N. J. Livesey, W. G. Read, J. W. Waters, E. V. Browell, J. W. Hair, M. A. Avery, T. J. McGee, L. W. Twigg, G. K. Sumnicht, K. W. Jucks, J. J. Margitan, B. Sen, R. A. Stachnik, G. C. Toon, P. F. Bernath, C. D. Boone, K. A. Walker, M. J. Filipiak, R. S. Harwood, R. A. Fuller, G. L. Manney, M. J. Schwartz, W. H. Daffer, B. J. Drouin, R. E. Cofield, D. T. Cuddy, R. F. Jarnot, B. W. Knosp, V. S. Perun, W. V. Snyder, P. C. Stek, R. P. Thurstans, and P. A. Wagner (2008), Validation of Aura Microwave Limb Sounder stratospheric ozone measurements, *J. Geophys. Res.*, 113, D15S20, doi:10.1029/2007JD008771.
- Imai, K., M. Suzuki, and C. Takahashi (2010), Evaluation of Voigt algorithms for the ISS/JEM/SMILES L2 data processing system, *Advances in Space Research*, doi: 10.1016/j.asr.2009.11.005.
- Imai, K., N. Manago, C. Mitsuda, Y. Naito, E. Nishimoto, T. Sakazaki, M. Fujiwara, L. Froidevaux, T. von Clarmann, G. Stiller, M. Donal, P. Rong, G. M. Martin, K. A. Walker, D. Kinnison, H. Akiyoshi, T. Nakamura, T. Miyasaka, T. Nishibori, S. Mizobuchi, K. Kikuchi, H Ozeki, C. Takahashi, H. Hayashi, T. Sano, M. Suzuki, M. Takayanagi and M. Shiotani, 2013a, Validation of ozone data from the Superconducting Submillimeter-Wave Limb-Emission Sounder (SMILES), J. Geophys. Res. Atmos., Accepted.
- Imai, K., M. Fujiwara, M. Suzuki, N. Manago, T. Sano, C. Mitsuda, Y. Naito, and M. Shiotani, 2013b, Comparison of ozone profiles between Superconducting Submillimeter-Wave Limb-Emission Sounder (SMILES) and worldwide ozonesonde measurements, *J. Geophys. Res. Atmos.*, submitted.
- Kikuchi K., T. Nishibori, S. Ochiai, H. Ozeki, Y. Irimajiri, Y. Kasai, M. Koike, T. Manabe, K. Mizukoshi, Y. Murayama, T. Nagahama, T. Sano, R. Sato, M. Seta, C. Takahashi, M. Takayanagi, H. Masuko, J. Inatani, M. Suzuki, and M. Shiotani (2010a), Overview and early results of the Superconducting Submillimeter-Wave Limb-Emission Sounder (SMILES), *J.*



- Geophys. Res., 115, D23306, doi:10.1029/2010JD014379.
- Kikuchi K., T. Nishibori, S. Ochiai, T. Manabe, H. Ozeki, R. Sato, T. Sano, Y. Irimajiri, and M. Shiotani (2010b), Instrument Overview and Operation of JEM/SMILES, *Proc. International Activities of the Photogrammetry, Remote Sensing and Spatial Information Science (ISPRS) Technical Commission VIII Symposium*, p. 100.
- Kunz, A., L. L. Pan, P. Konopka, D. E. Kinnison, and S. Tilmes (2011), Chemical and dynamical discontinuity at the extratropical tropopause based on START08 and WACCM analyses, *J. Geophys. Res.*, 116, D24302, doi:10.1029/2011JD016686.
- Kuwahara, T., T. Nagahama, H. Maezawa, Y. Kojima, H. Yamamoto, T. Okuda, N. Mizuno, H. Nakane, Y. Fukui and A. Mizuno (2012) Ground-based millimeter-wave observation of stratospheric ClO over Atacama, Chile in the mid-latitude Southern Hemisphere; *Atmos. Meas. Tech.*, 5, 2601–2611, doi:10.5194/amt-5-2601-2012.
- Livesey, N. J., W. Van Snyder, W. G. Read, and P. A. Wagner. Retrieval algorithms for the EOS Microwave Limb Sounder (MLS) (2006), *IEEE Trans. Geosci. Remote Sens.*, 44(5):1144–1155.
- Manago, N., M. Suzuki, C. Mitsuda, K. Imai, M. Yamada, S. Takehiro and M. Shiotani (2013), SMILES retrieval using Tikhonov regularization and Non-voigt line shape, *Proc. of atmosphere symposium* (written in Japanese)
- Mitsuda, C., M. Suzuki, Y. Iwata, N. Manago, Y. Naito, C. Takahashi, K. Imai, E. Nishimoto, H. Hayashi, M. Shiotani, T. Sano, M. Takayanagi, and H. Taniguchi (2011), Current status of level 2 product of Superconducting Submillimeter-Wave Limb-Emission Sounder (SMILES), *Proc. SPIE* 8176, 81760M.
- Mizobuchi, S., K. Kikuchi, S. Ochiai, T. Nishibori, T. Sano, K. Tamaki, and H. Ozeki (2012), In-orbit Measurement of the AOS (Acousto-Optical Spectrometer) Response Using Frequency Comb Signals, *IEEE Journal of Selected Topics in Applied Earth Observations and Remote Sensing*, **5** (3), 977-983, DOI:10.1109/JSTARS.2012.2196413.
- Ochiai, S., K. Kikuchi, T. Nishibori, T. Manabe, H. Ozeki, K. Mizukoshi, F. Ohtsubo, K. Tsubosaka, Y. Irimajiri, R. Sato, and M. Shiotani (2010), Performance of JEM/SMILES in orbit, 21th Int'l Symp. *Space Terahertz Technol.*, S8.1, (Oxford, UK), March 2010.
- Ochiai, S., K. Kikuchi, T. Nishibori, T. Manabe (2012), Gain Nonlinearity Calibration of Submillimeter Radiometer for JEM/SMILES, *IEEE Journal of Selected Topics in Applied Earth Observations and Remote Sensing*, 5(3), 962-969, doi:10.1109/JSTARS.2012.2193559.
- Pickett, H. M., R. L. Poynter, and E. A. Cohen (1992), Submillimeter, millimeter, and microwave spectral line catalogue. Technical Report JPL Publication 80-23, Rev.3, JPL.
- Rienecker, M. M., M.J. Suarez, R. Todling, J. Bacmeister, L. Takacs, H. -C. Liu, W. Gu, M. Sienkiewicz, R. D. Koster, R. Gelaro, I. Stajner, and J. E. Nielsen (2008), The GEOS-5 Data



- Assimilation System Documentation of Versions 5.0.1, 5.1.0, and 5.2.0, *NASA Technical Report Series on Global Modeling and Data Assimilation*, 27, NASA/TM-2008-104606.
- Rodgers, C. D. (1976), Retrieval of atmospheric temperature and composition from remote measurements of thermal radiation, *Rev. Geophys.*, 14(4), 609–624.
- Rodgers, C. D. (1990), Characterization and error analysis of profiles retrieved from remote sounding measurements, *J. Geophys. Res.*, 95(D5), 5587–5595.
- Rodgers, C. D. (2000), *Inverse Methods for Atmospheric Sounding: Theory and Practice, Ser. on Atmos., Oceanic, and Planet. Phys.*, vol. 2, World Scientific, Singapore.
- Rothman, L. S. et al. (2009), The HITRAN 2008 Molecular Spectroscopic Database, *J. Quant. Spectrosc. Radiat. Transfer* 110, 533–572, doi:10.1016/j.jqsrt.2009.02.013.
- Sakazaki T., M. Fujiwara, C. Mitsuda, K. Imai, N. Manago, Y. Naito, T. Nakamura, H. Akiyoshi, D. Kinnison, T. Sano, M. Suzuki, and M. Shiotani (2013), Diurnal ozone variations in the stratosphere revealed in observations from the Superconducting Submillimeter-Wave Limb-Emission Sounder (SMILES) onboard the International Space Station (ISS), *J. Geophys. Res.*, in press.
- Smith, A. K., V. L. Harvey, M. G. Mlynczak, B. Funke, M. García-Comas, M. Hervig, M. Kaufmann, 6 E. Kyrölä, M. López-Puertas, I. McDade, C. E. Randall, J. M. Russell III, P. E. Sheese, M. Shiotani, W. R. Skinner, M. Suzuki, K. A. Walker (2013), Satellite Observations of Ozone in the Upper Mesosphere, *J. Geophys. Res.*, under revision.
- Stachnik, R. A., L. Millán, R. Jarnot, R. Monroe, C. McLinden, S. Kühl, J. Puķīte, M. Shiotani, M. Suzuki, Y. Kasai, F. Goutail, J. P. Pommereau, M. Dorf, and K. Pfeilsticker (2013), "Stratospheric BrO abundance measured by a balloon-borne submillimeterwave radiometer", *Atmos. Chem. Phys.*, 13, 3307-3319, doi:10.5194/acp-13-3307-2013.
- Suzuki, M., C. Mitsuda, K. Kikuchi, T. Nishibori, S. Ochiai, H. Ozeki, T. Sano, S. Mizobuchi, C. Takahashi, N. Manago, K. Imai, Y. Naito, H. Hayashi, E. Nishimoto, M. Shiotani (2012), Overview of the Superconducting Submillimeter-Wave Limb-Emission Sounder (SMILES) and Sensitivity to Chlorine Monoxide, ClO, *IEEJ Transactions on Fundamentals and Materials*, 132, 8, 609-615, doi:10.1541/ieejfms.132.609.
- Takahashi, C., S. Ochiai, and M. Suzuki (2010), Operational retrieval algorithms for JEM/SMILES level 2 data processing system, *J. Quant. Spectrosc. Radiat. Transfer*, 111, 160–173.
- Takahashi, C., M. Suzuki, C. Mitsuda, S. Ochiai, N. Manago, H. Hayashi, Y. Iwata, K. Imai, T. Sano, M. Takayanagi, M. Shiotani (2011), Capability for ozone high-precision retrieval on JEM/SMILES observation, *Advances in Space Research*, v48, p1076-1085.



APPENDIX

A. 1. INFORMATION IN THE PREVIOUS VERSIONS

A. 1. 1. DESCRIPTION OF V1.0 (005-06-0024)

V1.0 is a test version in order to check L2 processing algorithms designed before launch [*Takahashi et al.*, 2010]. V1.0 gave priority to quality rather than quantity and 46 % of L1B files which had some kind of error status were not processed.

- The tangent altitude (geometrical) is calculated by using a) SMILES Star Sensors, b) SMILES scan mirror angle, and c) ISS position. SMILES Star Sensor shows unexpected large scattered output. We smoothed out the SMILES tangent altitude by second order fitting in this version. The tangent altitude precision should be 100 m (1 sigma) in rms according to the specifications which are now under verification.
- The two SMILES Star Sensors are pointing in fairly close directions to each other therefore there is a possibility that the SMILES tangent point cannot be calculated when both the sensors are within 45° of the Sun. In this situation, no L2 product is processed.
- The condition of vertical correlation is not introduced in the retrieval of any species except temperature, according to the results of the vertical correlation study.

A. 1. 2. IMPROVEMENTS IN V 1.1 (005-06-0032) UPDATE

• The goal of v1.1 is to increase the amount of useful data for creating gridded data using STT-ISS hybrid pointing data. The pointing direction for determining tangent altitudes is calculated by using SMILES scan mirror angle and ISS position. However, since pointing accuracy will heavily affect tangent altitude determination errors and an average altitude within a single scan is retrieved using the SMILES Star Sensor in L2 processing. In the case that sunlight or moonbeams enter the FOV of the SMILES Star Sensor, positioning information cannot be obtained, so this will be estimated from the information of 50 scans before and after the scan in question.

A. 1. 3. IMPROVEMENTS IN V 1.2 (005-06-0150) UPDATE

The goal of v1.2 is to suppress internal inconsistency between receivers. SMILES has 2 receivers (units 1 and 2) and response functions are fitted with the sum of triple-Gaussian functions based on

JEM/SMILES L2 Product Guide for v2.4



ground test data. However, these functions are not correct and mesospheric O₃, HCl and temperature have differences of 10-20 % between receiver units 1 and 2. We include experimental correction factors for the functions which determine that retrieved temperatures agree with TIMED/SABER.

- Illegal values in longitude when the longitude of the tangent point is around 180 degrees have been corrected.
- Altitude offset of Star Trackers (STT) has been reduced to +/- 1km due to the implementation of a compensation formula for time from STT.
- Rate of convergence in the retrieval process has been improved by smoothing vibrations in the ISS altitude data which do not seem to represent actual vibrations.
- Description of line shape has been refined with introducing the coefficient (v/v_0) .
- Line parameters of O₃, HNO₃, HO₂ and ozone isotopes have been changed from the JPL catalog to HITRAN2008.
- Profiles of temperature and HCl around 50km have been improved, with the compensation of an effect from the Doppler shift.
- Consistency between retrieval results from Band A in Setting 2 (Bands A/C) and Setting 3
 (Bands B/A) have been improved by compensating between the response functions of AU1 and AU2 (2 units in AOS).
- Hydrostatic assumption has been introduced as a constraint in the calculation of pressure and temperature.
- Retrieval results of HOCl have been improved by ignoring ozone isotopes whose absorption lines overlap that of HOCl in Band A.
- Information contents of ozone isotopes, HNO₃, ClO and CH₃CN have been increased by adjusting the error value in the *a priori* profile.
- Rate of convergence in the retrieval process has been increased by ignoring temperature retrieval in Band C.
- Rate of convergence in the retrieval process has been increased by raising the upper limit of iteration trials in the retrieval process from 5 to 8.

A. 1. 4. IMPROVEMENTS IN V 1.3 (006-06-0200) UPDATE

In this version, determination of screening flags and overall algorithm have been slightly modified. Mainly changes that have a physical basis have been adopted as it is assumed that these modifications can significantly affect the retrieved profiles with the implementation of the next planned update of L1B data processing.

- L1B data has been updated from version 005 to version 006.
 - > Retrieved profiles from scans near "FOV interference" were improved by referring to "the



flags indicating FOV disturbance." For details of the L1B data update, see the document "Level 1 Product Release Notes (Ver.006)".

- Standard temperatures for Lorentz width of absorption lines of O₃, HNO₃, HO₂ and ozone isotopes have been corrected from 300K to 296K. The effect of this correction is around a few percent.
- In correcting the tangent height on the observation point, antenna elevation offset introduction is retrieved from the average of altitude offset within one scan. According to this change, O₃ and HCl above 50km increase by a few percent.
- Antenna movement within the time to acquire a spectrum for single height is taken into account
 with the antenna pattern. This improvement causes an increase of a few percent in ozone at the
 peak height (lower stratosphere).
- In order to make better fitting of the curved baseline of brightness temperature, the uncertainty
 of absorption coefficient is fitted with a 2-dimensional function instead of its original
 1-dimensional function. As a result, baseline residue has been decreased by around half in
 comparison with the previous version.
- Regularization of status vectors in the inversion model with a priori errors has been introduced.
 Due to this improvement, 2-dimensional terms of the absorption coefficients with a small number of digits can be retrieved.
- The grids of retrieval altitude have been adjusted by 2, 3 or 4 km depending on species, band and altitude, instead of the uniform 3km in the previous version. In adjusting the altitude grid, the information of altitude resolution is referred to. As a result of this modification, species with high sensitivity (such as O₃ and HCl) can be retrieved on a more precise altitude grid, and those with low sensitivity (such as BrO and HO₂) can be retrieved with a wider altitude range.
- Altitude correlation of 10km has been introduced for all species except O₃ from Bands A and B.
- Information on convergence, FOV interference and observation altitude are stored in the *status* field. For details, see the format sheet in the Product Guide of v1.3.
- Information in order to evaluate spectrum residue, cost function for all species and all altitudes
 is stored in the CostFunctionY and CostFunctionYAll fields in the products.
- Bugs in the Averaging Kernel, Information Value and Vertical Resolution fields have been fixed.
- Preliminary "status flag" has been newly added from this version onwards.
- For the retrieval of Band C, a priori values for the tangent altitude are provided from Bands A
 or B. (There are operational modes with Bands A+C and Bands B+C.)

A. 1. 5. IMPROVEMENTS IN V 2.0 (007-08-0300) UPDATE



The objective of this update is to improve temperature profiles. L1B data has been updated to version 007 in which non-linear correction has been newly implemented. In this version, biases in stratospheric temperature have been suppressed and therefore O3 amounts decreased by 8% at the peak altitude. [Mitsuda et al., 2011]

- L1B data has been updated from version 006 to 007.
 - ➢ Gain nonlinearity correction has been applied to observed spectra [Ochiai et al., 2011). In the middle stratosphere, retrieved temperatures become closer to those of the Goddard Earth Observing System-5 assimilated data. Nonlinearity effects influence not only temperature but also other molecules. For those species such as O₃, HCl and ClO with strong lines the retrieved values decrease by 5 − 7% at 25 − 45 km. For those species such as HOCl and BrO with weak lines located at the wing of strong lines, the retrieved values change from around 50 − 100 %. In v1.3, the retrieved profiles of HOCl contained negative values at around 30km, but this has now been improved.
- A new AOS response function has been introduced. This function was modeled on new on-orbit measurement data for AOS response function in January of 2011 [Ozeki et al., 2011).
- Temperature field in the mesosphere is very sensitive to retrieval results, but retrieved temperature profiles above 40-50 km were not so good. Thus MLS temperature products (v2.2) to which the migrating tidal model (Global Scale Wave Model) was applied were referred to as the mesospheric temperature field.
- Preliminary corrections in observed frequency grids have been introduced. By removing frequency fitting residue in L1B data, residue in general decreases from 100 kHz to 50 kHz.
- Some line parameters have been updated (see Table A.1-1).
- Bugs in frequency grids around O¹⁷OO (Band B) and ¹⁸OOO (Band C) have been fixed. This update reduces systematic errors above 50km.

Table A.1-1 Updated line parameters in v2.0

Para	ameters	L2 v1.3	v2.0	Reference
O_3				
-	Line position	624371.112	624371.223	Ozeki, private communications
	(MHz)			(preliminary results)
-	γ_0 (MHz/hPa)	2.258	2.3078	HITRAN2008
-	$n_{_{\scriptscriptstyle \gamma}}$	0.77	0.78	HITRAN2008
H ³⁵ (Cl			
-	Line position	625901.603	625901.6584	MASTER
	(MHz)	625918.756	625918.6975	
		625932.007	625932.0081	
-	γ_0 (MHz/hPa)	2.57	2.541	MLS Forward model ATBD (v1.0)
-	$n_{_{\scriptscriptstyle \gamma}}$	0.73	0.723	MLS Forward model ATBD (v1.0)



Par	ameters	L2 v1.3	v2.0	Reference
H ³⁷	CI			
-	Line position	624964.374	624964.3694	MASTER
	(MHz)	624977.821	624977.8013	
		624988.334	624988.2821	
-	γ_0 (MHz/hPa)	2.57	2.541	MLS Forward model ATBD (v1.0)
-	$n_{_{\scriptscriptstyle \gamma}}$	0.73	0.723	MLS Forward model ATBD (v1.0)
ClO)			
-	Line position	649445.040	649445.250	Oh and Cohen, 1994
	(MHz)	649451.170	649451.072	
¹⁸ O	00			
-	Line position	649137.611	649137.132	Ozeki, private communications
	(MHz)	649137.611	649137.132	(preliminary results)
		649149.603	649152.038	
		649152.601	649152.038	

A. 1. 6. IMPROVEMENTS IN V 2.1(007-08-0310) UPDATE

The HOCl product was improved in v2.1. Other products such as O₃ have not been changed.

 Some line parameters have been updated (see Table A.1-2). HOCl spectral lines are located at the shoulder of these lines. Residual spectra around HOCl were suppressed.

	•	•	
Parameters	L2 v2.0	v2.1	Reference
$O_{3(v1,3)}$ (625012.89 MHz)			
- γ_0 (MHz/hPa)	2.3078	2.017	HITRAN 2008
$-n_{\nu}$	0.78	0.76	
$O_{3(v1,3)}'$ (625051.27 MHz)			
- γ_0 (MHz/hPa)	2.3078	2.172	
$-n_{\nu}$	0.78	0.79	
¹⁸ OOO			
 Line position (MHz) 	625088.260	625090.4623	JPL catalog
	625091.258	625091.8080	

Table A.1-2 Updated line parameters in v2.1

A. 1. 7. IMPROVEMENTS IN V 2.2 (007-09-0400) UPDATE

The objectives of this version are improvements in retrieval in the mesosphere and vibrations in the profile. In order to resolve these problems, the following improved points have been adopted:

• Altitude range of retrieval has been extended. In addition, the altitude ranges are independently modified by species (e.g. Upper limit of retrieval was 85km for all species in the previous version but it has been extended up to 100km for O₃, HCl and HO₂ whose sensitivity is relatively high). Moreover, *a priori* errors for BrO, HO₂, and O₃ isotopes have been widened in comparison to the previous version. This has resulted in the presence of an HO₂ peak in the



- lower thermosphere at night-time.
- The inversion algorithm has been modified in order to suppress vibrations in the profiles. For the retrieval of O₃, HCl and HNO₃, Tikhonov Regularization has been implemented in combination with the Optical Estimation Method. (Manago et al., 2013)
- AOS response function has been revised. Although the data referred to in the retrieval process
 is still that of the same orbit as the previous version, another analytic method for modeling
 weaker signals has been adopted. (Mizobuchi et al., 2012)
- Spectral line parameters for O₃ and its isotopes have been modified. The preliminary results of a new measurement experiment have been replaced with certified values. For ¹⁸OOO in Band B, the parameters have been also replaced from HITRAN2008 [Rothman et al., 2009] with JPL Catalog [Pickett et al., 1992] (see Table A.1-3). As a result, the spectrum residual has been significantly improved.
- Some other minor changes have been implemented:
 - For a priori profiles of HOCl, climatological data generated from Aura/MLS v2.2 has been replaced with CCSR/NIES climatological data.
 - A formula for gravity acceleration in the Forward model has been modified so that the Geodetic Reference System 1980 has been adopted uniformly in the L2 retrieval system.
 - For altitudinal interpolation of pressure data in *a priori* datasets, a linear interpolation of logarithm of pressure has been adopted instead of a linear interpolation of pressure.
 - > Some programming bugs have been fixed.
 - ♦ Mistakes in standard temperature for spectral line parameters of HCl have been fixed.

Table A.1-3 Line parameter updates in v2.2

Parameters	L2 v2.1	v2.2	Reference
O ₃ - Line position (MHz)	624371.223	624371.242	Ozeki, private communications
H ³⁵ Cl			
- γ_0 (MHz/hPa)	2.541	2.566	MLS Forward model ATBD (v1.0)
H ³⁷ Cl			
- γ_0 (MHz/hPa)	2.541	2.566	MLS Forward model ATBD (v1.0)



Parameters	L2 v2.1	v2.2	Reference
¹⁸ OOO (band B)			
- Line position	-	625387.9462	JPL catalog
(MHz)	625564.930	625563.6585	
	625939.671	625939.4177	
- log10(Intensity)	-	-5.502000	
(nm ² MHz)	-3.463879	-3.428500	
	-3.858954	-3.825100	
- γ_0 (MHz/hPa)	-	2.1488	
	2.1488	2.1488	
	2.1219	2.1488	
$-n_{\gamma}$	-	0.79	
,	0.79	0.79	
	0.81	0.79	
¹⁸ OOO (band C)	649137.132	649137.167	Ozeki, private communications
- Line position	649137.132	649138.651	
(MHz)	649152.038	649152.004	
	649152.038	649152.004	

A. 1. 8. IMPROVEMENTS IN V 2.3 (007-09-0402) UPDATE

In this version, the retrieval algorithm is the same as that of v2.2, and some product data and flags have been improved.

- Datasets which interpolated with pressure grid data have been added. This grid data is uniform throughout all species.
- The definition of status flag has been modified and therefore that percentage of available scan data has exceeded 80% for all observation bands. Screening with convergence conditions has been relaxed, while screening with spectrum fitting has been newly introduced. Quality information for HCl profiles has been reflected in status flags for indicating FOV interference, instead of flags of FOV interference from L1B data. Quality information will have error values if an HCl profile runs out of variance for profile zonal means 5 times.

A. 1. 9. IMPROVEMENTS IN V 2.4 (008-11-0502) UPDATE

The objectives of this version are improvements in thermospheric O_3 and HCl and mesospheric HCl. Other than the modifications described in Section 3, some other points have been adopted:

- L1b data has been updated to version 008. In this version, non-linear correction factors and information for tangent height have been revised. [Ochiai et al., 2012]
- A priori and its errors for O3 and HCl have been modified in order to extend the available altitude range for retrieval process up to the lower thermosphere.
- GEOS-5 dataset, which is used as an a priori for the meteorological field, has been revised by nudging with temperature and O₃ data from MLS observation, which resulted in the improvement of mesospheric temperature in the dataset. For the *a priori* of temperature profiles



in the v2.4 algorithm, GEOS-5 is referred up to 70km, and the nearest grid of Aura/MLS data is referred to at a higher altitude. Tidal correction of Aura/MLS data with GSWM has been suspended. As a result of these modifications, the variance of mesospheric HCl which depends on temperature variation has been suppressed.

- The frequency of spectral lines of O₃, excited O₃ and O₃ isotopes have been re-measured in laboratory experiments (see Table A.1-4). [Ozeki, private communication] As a result of this modification, the peak amount of HOCl has changed by around 10%, whose spectral line is positioned at the shoulder of these O₃.
- For a priori profiles, climatological data from UARS/MLS data has been replaced with the calculation results from the nearest grid from SD-WACCM.

Table A.1-4 Line parameter updates in v2.4

			ne parameter u	
Para	ameters	L2 v2.3	v2.4	Reference
O_3				
-	Line position	624371.242	625371.2411	Ozeki, private communications
	(MHz)	625894.872	625894.8670	
O _{3(v.}	2)			
- `	Line position	625280.7683	625280.6315	Ozeki, private communications
	(MHz)	625324.0214	625324.2100	
O _{3(v}	1,3)			
- `	Line position	625051.274	625051.3218	Ozeki, private communications
	(MHz)			
O ¹⁷ (00			
-	Line position	625770.858	625770.914	Ozeki, private communications
	(MHz)	625770.918	625770.974	
		625771.308	625771.364	
		625771.757	625771.813	
		625771.787	625771.843	
		625771.877	625771.933	
		625772.027	625772.083	
		625772.117	625772.173	
		625772.147	625772.203	
		625772.177	625772.233	
		625772.177	625772.233	
		625772.357	625772.413	
		625772.477	625772.533	
		625772.986	625773.042	
		625773.046	625773.102	
		625773.496	625773.552	
		625781.950	625782.027	
		625782.010	625782.087	
		625782.400	625782.477	
		625782.850	625782.927	
		625782.880	625782.957	
		625782.910	625782.987	
		625783.089	625783.166	
		625783.179	625783.256	
		625783.209	625783.286	



Parameters	L2 v2.3	v2.4	Reference
	625783.239	625783.316	
	625783.239	625783.316	
	625783.419	625783.496	
	625783.569	625783.646	
	625783.989	625784.066	
	625784.109	625784.186	
	625784.528	625784.605	
	625868.740	625868.897	
	625868.770	625868.927	
	625869.130	625869.287	
	625869.400	625869.557	
	625869.550	625869.707	
	625869.669	625869.826	
	625869.729	625869.886 625869.976	
	625869.819		
	625869.909	625870.066	
	625869.939	625870.096	
	625869.969	625870.126	
	625869.969	625870.126	
	625870.329	625870.486	
	625870.389	625870.546	
	625870.749	625870.906	
	625870.989	625871.146	
	626086.269	626086.346	
	626086.299	626086.376	
	626086.689	626086.766	
	626087.139	626087.216	
	626087.139	626087.216	
	626087.169	626087.246	
	626087.349	626087.426	
	626087.469	626087.546	
	626087.469	626087.546	
	626087.529	626087.606	
	626087.529	626087.606	
	626087.649	626087.726	
	626087.858	626087.935	
	626088.188	626088.265	
	626088.368	626088.445	
	626088.728	626088.805	
	626315.311	626315.353	
	626315.401	626315.443	
	626315.791	626315.833	
	626316.240	626316.282	
	626316.300	626316.342	
	626316.420	626316.462	
1	626316.510	626316.552	
	626316.600	626316.642	
	626316.660	626316.702	
	626316.660	626316.702	
	626316.690	626316.732	
	626316.870	626316.912	
	626316.960	626317.002	
	626317.529	626317.571	



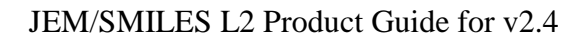
Parameters	L2 v2.3	v2.4	Reference
Tarameters	626317.529	626317.571	Reference
	626318.039	626318.081	
	649793.407	649793.493	
	649793.587	649793.673	
	649793.857	649793.943	
	649794.307	649794.393	
	649794.367	649794.453	
	649794.667	649794.753	
	649794.667	649794.753	
	649794.696	649794.782	
	649794.726	649794.812	
	649794.786	649794.872	
	649794.906	649794.992	
	649794.996	649795.082	
	649794.996	649795.082	
	649795.656	649795.742	
	649795.746	649795.832	
	649796.315	649796.401	
¹⁷ 000			
- Line position	625009.205	625009.882	Ozeki, private communications
(MHz)	625009.235	625009.912	
	625009.535	625010.212	
	625009.565	625010.242	
	625009.595	625010.272	
	625009.715	625010.392	
	625009.775	625010.452	
	625009.805	625010.482	
	625009.895	625010.572	
	625010.075	625010.752	
	625010.164	625010.841	
	625010.284	625010.961	
	625010.374	625011.051	
	625010.644	625011.321	
	625010.944	625011.621	
	625011.514	625012.191	
	649274.647	649274.532	
	649274.856	649274.741	
	649274.946	649274.831	
	649275.216	649275.101	
	649275.276	649275.161	
	649275.546	649275.431	
	649275.606	649275.491	
	649275.696	649275.581	
	649275.756 649275.786	649275.641	
		649275.671	
	649275.846 649275.846	649275.731 649275.731	
	649275.936	649275.821	
	649276.325	649276.210	
	649276.745	649276.630	
	649276.985	649276.870	
	649969.595	649969.474	
	649969.805	649969.684	
	UT//U/.0UJ	UT//U/.UU 1	



Parameters	L2 v2.3	v2.4	Reference
	649969.895	649969.774	
	649970.105	649969.984	
	649970.195	649970.074	
	649970.465	649970.344	
	649970.495	649970.374	
	649970.615	649970.494	
	649970.675	649970.554	
	649970.705	649970.584	
	649970.765	649970.644	
	649970.765	649970.644	
	649970.765	649970.644	
	649971.244	649971.123	
	649971.634	649971.513	
	649971.874	649971.753	
	649980.298	649980.295	
	649980.628	649980.625	
	649980.628	649980.625	
	649980.988	649980.985	
	649981.167	649981.164	
	649981.317	649981.314	
	649981.347	649981.344	
	649981.407	649981.404	
	649981.437	649981.434	
	649981.527		
	649981.557	649981.524	
	649981.587	649981.554	
	649981.857	649981.584	
	649981.977	649981.854	
	649982.457	649981.974 649982.454	
	649982.876	649982.873	
	650009.498	650009.549	
	650009.828	650009.879	
	650009.858	650009.879	
	650010.187	650010.238	
	650010.187	650010.238	
	650010.547	650010.598 650010.628	
	650010.577 650010.637		
	650010.667	650010.688	
		650010.718	
	650010.727	650010.778 650010.838	
	650010.787		
	650010.817	650010.868	
	650011.087	650011.138	
	650011.177	650011.228	
	650011.686	650011.737	
1	650012.106	650012.157	
	650041.456	650041.458	
	650041.755	650041.757	
	650041.785	650041.787	
	650042.145	650042.147	
	650042.265	650042.267	
	650042.445	650042.447	
	650042.505	650042.507	



Parameters	L2 v2.3	v2.4	Reference
	650042.535	650042.537	
	650042.595	650042.597	
	650042.685	650042.687	
	650042.715	650042.717	
	650042.745	650042.747	
	650042.955	650042.957	
	650043.105	650043.107	
	650043.614	650043.616	
	650044.004	650044.006	
	650158.585	650158.676	
	650158.944	650159.035	
	650158.974	650159.065	
	650159.304	650159.395	
	650159.544	650159.635	
	650159.664	650159.755	
	650159.694	650159.785	
	650159.754	650159.845	
	650159.784	650159.875	
	650159.844	650159.935	
	650159.904	650159.995	
	650159.964	650160.055	
	650160.233	650160.324	
	650160.293	650160.384	
	650160.833	650160.924	
	650161.253	650161.344	
	650166.859	650166.808	
	650167.129	650167.078	
	650167.159	650167.108	
	650167.488	650167.437	
	650167.608	650167.557	
	650167.818	650167.767	
	650167.878	650167.827	
	650167.878	650167.827	
	650167.938	650167.887	
	650168.028	650167.977	
	650168.088	650168.037	
	650168.088	650168.037	
	650168.298	650168.247	
	650168.478	650168.427 650168.906	
	650168.957 650169.317		
	650169.317 650333 813	650169.266	
	650333.813 650334.083	650333.882 650334.152	
	650334.113 650334.443	650334.182 650334.512	
	650334.533	650334.602	
	650334.743	650334.812	
	650334.743	650334.872	
	650334.833	650334.872	
	650334.893	650334.962	
	650334.893	650335.051	
	650335.042	650335.031	
	650335.042	650335.111	





Parameters	L2 v2.3	v2.4	Reference
	650335.192	650335.261	
	650335.432	650335.501	
	650335.912	650335.981	
	650336.242	650336.311	
¹⁸ OOO	_		
- Line position	625090.4623	625089.9539	Ozeki, private communications
(MHz)	625091.8080	625091.3796	
	625563.6585	625563.6906	
	625939.4177	625939.4927	
	649137.167	649137.1577	
	649138.651	649138.7454	
	649152.004	649151.6253	
	649152.004	649152.4312	



A. 2. Sample of source code for reading L2 product (in python)

A sample python code is shown below.

```
#!/usr/bin/env python
# import normal libraries.
import os
import sys
import numpy as np
# import HDF5 library
import h5py
print "Process Start -----"
# set HDF file
fnam = 'dir/008-11-0502/A/2009/10/12/SMILES_L2_03_A_008-11-0502_20091012.he5'
# open HDF file
if os.path.exists(fnam):
   f = h5py.File(fnam,'r')
else:
   print 'File does not exist: %s'%(fnam)
   sys.exit()
# read HDF fields
L2Val=np.array(f['/HDFEOS/SWATHS/03/Data Fields/L2Value'])
L2Prc=np.array(f['/HDFEOS/SWATHS/03/Data Fields/L2Precision'])
L2Flg=np.array(f['/HDFEOS/SWATHS/03/Data Fields/Status'])
L2Tim=np.array(f['/HDFEOS/SWATHS/03/Geolocation Fields/Time'])
L2Alt=np.array(f['/HDFEOS/SWATHS/03/Geolocation Fields/Altitude'])
# change array's shape (timexaltitude)
L2Val=L2Val.reshape(len(L2Tim),len(L2Alt))
L2Prc=L2Prc.reshape(len(L2Tim),len(L2Alt))
# set scan screening condition
cnd = (L2Flg == 0)
# scan loop (screened)
for i in range(len(L2Tim[cnd])) :
   print 'LOOP %i -----'%(i)
   # print L2 data and precision.
   # However, if this data is unuseful, print "-999.99".
   for j in range((len(L2Alt))) :
```

